



**British
Geological Survey**

NATURAL ENVIRONMENT RESEARCH COUNCIL

Multiphase water-escape features developed in glacial sediments exposed at Clava, Inverness

Physical Hazards Programme

Internal Report IR/07/12

BRITISH GEOLOGICAL SURVEY

PHYSICAL HAZARDS PROGRAMME

INTERNAL REPORT IR/07/12

Multiphase water-escape features developed in glacial sediments exposed at Clava, Inverness

Emrys Phillips

Contributor

Jon Merritt

The National Grid and other Ordnance Survey data are used with the permission of the Controller of Her Majesty's Stationery Office.
Licence No: 100017897/2005.

Keywords

Micromorphology, water-escape, glacial sediments, Inverness.

Bibliographical reference

PHILLIPS, E.R. 2006. Multiphase water-escape features developed in glacial sediments exposed at Clava, Inverness. *British Geological Survey Internal Report, IR/07/12*. 35pp.

Copyright in materials derived from the British Geological Survey's work is owned by the Natural Environment Research Council (NERC) and/or the authority that commissioned the work. You may not copy or adapt this publication without first obtaining permission. Contact the BGS Intellectual Property Rights Section, British Geological Survey, Keyworth, e-mail ipr@bgs.ac.uk. You may quote extracts of a reasonable length without prior permission, provided a full acknowledgement is given of the source of the extract.

Maps and diagrams in this book use topography based on Ordnance Survey mapping.

BRITISH GEOLOGICAL SURVEY

The full range of Survey publications is available from the BGS Sales Desks at Nottingham, Edinburgh and London; see contact details below or shop online at www.geologyshop.com

The London Information Office also maintains a reference collection of BGS publications including maps for consultation.

The Survey publishes an annual catalogue of its maps and other publications; this catalogue is available from any of the BGS Sales Desks.

The British Geological Survey carries out the geological survey of Great Britain and Northern Ireland (the latter as an agency service for the government of Northern Ireland), and of the surrounding continental shelf, as well as its basic research projects. It also undertakes programmes of British technical aid in geology in developing countries as arranged by the Department for International Development and other agencies.

The British Geological Survey is a component body of the Natural Environment Research Council.

British Geological Survey offices

Keyworth, Nottingham NG12 5GG

☎ 0115-936 3241 Fax 0115-936 3488

e-mail: sales@bgs.ac.uk

www.bgs.ac.uk

Shop online at: www.geologyshop.com

Murchison House, West Mains Road, Edinburgh EH9 3LA

☎ 0131-667 1000 Fax 0131-668 2683

e-mail: scotsales@bgs.ac.uk

London Information Office at the Natural History Museum (Earth Galleries), Exhibition Road, South Kensington, London SW7 2DE

☎ 020-7589 4090 Fax 020-7584 8270

☎ 020-7942 5344/45 email: bgs london@bgs.ac.uk

Forde House, Park Five Business Centre, Harrier Way, Sowton, Exeter, Devon EX2 7HU

☎ 01392-445271 Fax 01392-445371

Geological Survey of Northern Ireland, Colby House, Stranmillis Court, Belfast BT9 5BF

☎ 028-9038 8462 Fax 028-9038 8461

Maclean Building, Crowmarsh Gifford, Wallingford, Oxfordshire OX10 8BB

☎ 01491-838800 Fax 01491-692345

Columbus House, Greenmeadow Springs, Tongwynlais, Cardiff, CF15 7NE

☎ 029-2052 1962 Fax 029-2052 1963

Parent Body

Natural Environment Research Council, Polaris House, North Star Avenue, Swindon, Wiltshire SN2 1EU

☎ 01793-411500 Fax 01793-411501

www.nerc.ac.uk

Foreword

This report is the published product of a study by the British Geological Survey (BGS) as part of their strategic Physical Hazards Programme. It describes the micromorphology of a suite of glacial sediments from the Clava area, Inverness-shire, Scotland. The work forms part of a multidisciplinary Tills Engineering Geology Project.

Contents

Foreword	i
Contents	i
Summary	iii
1 Introduction	3
2 Quaternary geology of the Clava area	3
3 Macroscopic deformation structures	5
3.1 Hydrofractures.....	5
3.2 Thrusts and high strain zones.....	6
4 Micromorphology	7
4.1 Analytical techniques.....	7
4.2 Terminology.....	8
4.3 Thin section descriptions.....	8
5 Evidence of multiphase water-escape during deformation of the glaciogenic sediments at Clava	21
5.1 Thrusts and high strain zones.....	21
5.2 Hydrofracturing and layer-parallel flow zones in the Clava Sand Member.....	22
5.2.1 Event 1 - layer-parallel thrusting and associated deformation.....	22
5.2.2 Event 2 – repeated layer-parallel injection of fluidised sediment.....	23
5.2.3 Event 3 – development of the sand-filled water-escape conduit.....	24
5.2.4 Event 4 – main phase of hydrofracturing.....	25
Glossary	29
References	30

FIGURES

Figure 1. Simplified geological map of the Clava area showing the locations of the main sections studied (after Merritt, 1992). Insets - location maps.

Figure 2. Section through the Pleistocene glaciogenic sequence exposed in the ‘Main Pit’ (Merritt, 1992).

Figure 3. Section through the Pleistocene glaciogenic sequence exposed in the stream section to the west of Drummore of Clava (Section III of Merritt, 1992). The approximate locations of samples N4691 (QX194) and N4692 (QX195) are also shown.

Figure 4. Photographs of laminated sand, silt and clay filled hydrofractures cutting the Clava Sand Member, the ‘Main Pit’ section. (a) subhorizontal hydrofracture showing location of samples N4693 (QX196) and N4694 (QX197); (b) steeply dipping hydrofracture showing location of sample N4696 (QX200).

Figure 5. Photograph of a clay-rich high strain zone marking a thrust deforming the glaciofluvial deposits exposed in the stream section west of Drummore of Clava. The location of sample N4691 (QX194) is also shown.

Figure 6. Annotated scan of thin section N4691 (QX194) showing main structures developed within this deformed, laminated sand, silt and clay.

Figure 7. Annotated scan of thin section N4692 (QX195) showing main structures developed within this diamicton, Clava Shelly Till Member.

Figure 8. Annotated scan of thin section N4693 (QX196) showing main structures developed within this deformed, laminated sand, silt and clay, Clava Sand Member. Most prominent structure is a steeply dipping clay and silt-filled hydrofracture system.

Figure 9. Annotated scan of thin section N4694 (QX197) showing main structures developed within this deformed, laminated sand, silt and clay, Clava Sand Member.

Figure 10. Annotated scan of thin section N4695 (QX198) showing main structures developed within this deformed, laminated sand, silt and clay, Clava Sand Member. Most prominent structure is a steeply dipping sand, silt and clay-filled hydrofracture system.

Figure 11. Annotated scan of thin section N4696 (QX200) showing main structures developed within this deformed, laminated sand, silt and clay, Clava Sand Member. Most prominent structure is this highly brecciated sample is a funnel-shaped, steeply dipping sand, clay and silt-filled hydrofracture system.

TABLES

Table 1. Lithostratigraphy of the Pleistocene glaciogenic deposits exposed in the Clava area, near Inverness (Merritt, 1992). For location of sections see Figure 1.

Table 2. Details of samples collected from the stream section to the west of Drummore of Clava and Clava ‘Main Pit’.

Table 3. Possible correlations between the various deformation, hydrofracturing and liquefaction events recognised in samples N4693, N4694, N4695 and N4696 collected from Clava ‘Main Pit’.

Summary

This report describes the micromorphology of samples prepared from Quaternary glaciogenic sediments exposed in the Clava area, near Inverness, Scotland. The work forms part of the Engineering Geology of Tills Project of the Physical Hazards Programme.

The first part of the report provides the background information on the Quaternary geology of the Clava area. This is followed by a section describing the detailed micromorphology of six large format thin sections of the matrix of a locally shelly, clay-rich silty diamicton and the structurally overlying sands, silts and clay layers. The results are used to develop a model for the role of pressurised pore water and water-escape during the glacitectonic emplacement of rafts of shell-bearing marine deposits within the Pleistocene glaciogenic sequence exposed at Clava.

1 Introduction

This report describes the micromorphology of a sequence of deformed sands, silts and clays which form part of the Pleistocene glaciogenic sequence exposed in the Clava area, near Inverness, Scotland (Figure 1). The Quaternary geology of this area has been of significant interest since the nineteenth century when a bed of clay containing cold water marine shells were discovered beneath a till in a clay pit [NH 7658 4411] at an altitude of 150 m above ordnance datum (O.D.) (Fraser, 1883; Peacock, 1975; Merritt, 1992). This shelly clay, like several other elevated shell-bearing deposits discovered elsewhere in Scotland at about the same time, has caused considerable controversy (see Gordon, 1990; Merritt, 1992). The debate has centred on whether the deposits were in situ and, therefore, represent a submergence of up to 160 m above O.D. prior to the last glaciation in Scotland, or whether some, if not all, were transported by ice (see Merritt 1992). The Pleistocene glaciogenic sediments, including the shelly deposits, were examined in detail by Peacock (1975) and Merritt (1992). Consequently the Quaternary geology of the Clava area is only summarised here. Merritt (1992) concluded that the Clava shelly clay, and several other discrete masses of Clava sand and shelly till, are glacially transported allochthonous rafts of sediment transported from the Great Glen.

Micromorphology is a relatively new and, currently, still developing technique and refers to the examination of unlithified Quaternary deposits and other glacial sediments in thin section (see van der Meer, 1987, 1993; Menzies, 2000). A total of six large format thin sections of sediment from the 'Main Pit' and Drummore of Clava stream section have been examined during this study. The results are used to develop a model for the emplacement of the rafts of marine sediments within the glaciogenic sequence exposed at Clava.

2 Quaternary geology of the Clava area

The Clava site (Figure 1) is located on the southeastern side of the valley of the River Nairn, approximately 9 km east of Inverness. Landforms in the area are dominated by a number of northeast–southwest-trending benches (up to *c.* 265 m O.D.) which slope gently towards the

centre of the Nairn valley, as well as down valley. These benches are not simple fluvial or glaciofluvial terraces, although many of the lower ones have been modified by glacial drainage in an ice marginal setting. The sections examined during this study all occur in one of these benches (Figure 1). The glaciogenic sediments exposed in these sections rest upon a bedrock comprising gravelly sandstones and conglomerates representing the basal part of the Middle Devonian Inverness Sandstone Group. These fluvial sedimentary rocks rest unconformably upon a basement of granitic igneous rocks and amphibolite facies metasedimentary and meta-igneous rocks.

The lithostratigraphy for the Clava area is shown in Table 1 (Merritt, 1992). Parts of this sequence are exposed in the ‘Main Pit’ [NH 7658 4411] (Figure 2) and the stream section [NH 7637 4369] west of Drummore of Clava (section III of Merritt, 1992) (Figure 3), and form the focus of the present study.

Table 1. Lithostratigraphy of the Pleistocene glaciogenic deposits exposed in the Clava area, near Inverness, taken from Merritt (1992). For location of sections see Figure 1.

Unit	Formation	Section			
		Main Pit	Finglack Section	Section III	Section VI
5	Finglack Till Formation				
	‘flow till’ facies				*
	‘basal melt-out till’ facies				*
	‘lodgement till’ facies	*	*	*	*
4	Glaciofluvial ice-contact deposits			*	?
3	Clava Shelly Formation				
3c	Clava Sand Member	*	?	*	
3b	Clava Shelly Clay Member	*	?		
3a	Clava Shelly Till Member		?	*	
2	Drummore Gravel Formation	*	*		
1	Cassie Till Formation	*		?	
	Inverness Sandstone Group bedrock	*		near	

The Cassie Till (Unit 1) has only been positively proven in boreholes and is described as a ‘brown clay with stones’ and has been interpreted as a pre-Late Devensian basal till (Merritt, 1992). This till is overlain by the Drummore Gravel (Unit 2) which comprises an at least 3 m thick sequence of crudely stratified, very poorly sorted and clayey gravel containing large blocks of sandstone (up to 0.5 m in length) derived from the underlying local bedrock. The Drummore Gravel is compositionally similar to the Finglack Till Formation exposed at the top of the sequence.

The Drummore Gravel is apparently overlain by the Clava Shelly Till Member (Unit 3a) of the Clava Shelly Formation (Table 1) at Finglack, although no shelly material has yet been reported. The contact with the underlying gravel is sharp. The till is best developed at Section III and in the stream bed downstream where it is a very stiff, fissile, matrix-supported diamicton with a silty fine-sandy clay matrix containing sparse shelly material. The till is crudely layered and contains rounded to well-rounded, pebble (Udden 1914) sized clasts of metasandstone (psammite), quartzite and semipelitic gneiss, as well as lesser amounts of granite and sandstone. At ‘Main Pit’, the Drummore Gravel Formation is overlain by the Clava Shelly Clay Member (Unit 3b), a 4.9 m thick unit of weakly stratified, bluish grey clay and silt containing thin, streaky

laminae of sand and thin beds of gravel. The basal 0.4 m of the Clava Shelly Clay Member contains well-rounded pebbles (Udden 1914) of micaceous gneiss, Old Red Sandstone and granite. The overlying silty clay (0.6 m thick) is stiff and deformed by closely spaced shears and small-scale faults. The uppermost metre of the shelly clay comprises poorly defined, graded beds of dark grey silty clay, clayey silt and very fine-grained sand.

The Clava Shelly Clay Member is conformably overlain by the fine-grained sands of the Clava Sand Member (Unit 3c, Table 1). This slightly micaceous, silty fine- to medium-grained sand unit is weakly laminated and locally contains well-rounded granules and pebbles (Udden 1914) of metasandstone. In the 'Main Pit' section the Clava Sand Member is directly overlain by Finglack Till Formation (Unit 5, Figure 2). The contact is marked by a 40 cm thick zone of highly deformed (thrusting, boudinage), overconsolidated silty fine-grained sand containing boudinaged lenses of diamicton, beds of coarse-grained pebbly sand and disrupted clasts of clay. In Section III, the upper contact of the Clava Sand Member is sharp and was interpreted by Merritt (1992) as being partially glacitectonic and partially erosional. The lower boundary of the Clava Sand Member is also glacitectonic and formed by a marked planar décollement surface. In this stream section, the Clava Sand Member can be divided into two; the lower part (2 m thick) of the Member being generally more thinly bedded and finer grained than the upper part. Soft-sediment deformation structures are common within the finer grained lower part of the Clava Sand Member.

The variably exposed Finglack Till Formation (Unit 5) comprises a thick (at least 8 m), massive unit of stiff, matrix-supported diamicton. Angular to well-rounded pebbles and cobbles are mainly composed of fine-grained sandstones and flagstones derived from the Inverness Sandstone Group, with some metasandstone, quartzite and sparse granite. The basal part of the unit in the Finglack section contains numerous, well-rounded pebbles derived from the underlying Clava Shelly Till Member. In Section VI, the uppermost 3 to 4 m of is composed of a very poorly sorted cobble gravel interbedded with thin, laterally discontinuous beds and laminae of silt, sand and fine gravel. These sediments show evidence of fluvial reworking, slumping and deposition by cohesive mass-flows. The lower part of this section is more massive comprising thick (up to 0.5 m) beds of diamicton interbedded with seams (up to 10 cm thick) of sand with erosive bases. Peacock (1975) interpreted the whole sequence as supraglacial flow tills. However, the basal part of the diamicton contains an arch-shaped lens of clast supported gravel, indicative of deposition within a channel/cavity in the sole of a melting/wet based ice-sheet (Merritt, 1992). The upper till exposed in Section III is relatively inaccessible, but has been correlated with the Finglack Till Formation (Merritt, 1992).

The unnamed glaciofluvial ice contact deposits (Unit 4) are exposed in the Section III only (Figure 3) and comprise by predominantly waterlain, poorly sorted, clast-supported gravels interbedded with pebbly medium- to coarse-grained sand. Subangular to well-rounded pebbles are mainly composed of micaceous metasandstone and semipelitic gneiss, sandstone and medium-grained granitic gneiss. Clasts of granite, porphyritic dacite to rhyolite, and felsite are rare.

3 Macroscopic deformation structures

3.1 HYDROFRACTURES

Merritt (1992) described a range of macroscopic structures deforming the Clava Sand and Clava Shelly Clay members exposed in the area of the 'Main Pit'. The most conspicuous features are a network of cross-cutting fractures or fissures filled by hard, finely interlaminated clay, silt and

fine-grained sand. The lamination within these pale to dark yellow-brown, fine-grained sediment fills occurs parallel to the sides of the veins. These sediment-filled fissures (now interpreted as hydrofractures) are composed of stacked, discrete graded beds (≤ 1.5 cm thick) of fine-grained sand and silt (≤ 15 cm thick), and can be traced laterally for at least 5 m (Figure 4). The main fissures appear to dip towards the east-southeast, with minor, anastomosing branches off these major hydrofracture systems dipping at 60° east-northeast. The subhorizontal hydrofractures occur parallel to bedding within the Clava Sand Member and have accommodated varying amounts of layer-parallel ductile shearing. The relationship of this shearing event to the deposition of the sediment fills within the hydrofractures is unclear on the macroscopic scale.

Merritt (1992) concluded that hydrofracturing was associated with an extensional brittle deformation event, which occurred whilst the Clava Sand Member was frozen. He interpreted the laminated fills in the fissures as recording the intermittent injection of subglacial or englacially derived meltwater, depositing the clastic material before the fissures could close or the surrounding sediment could thaw. This deformation event may have occurred whilst the sediments were being overridden by ice, or as they were being incorporated into the glacier as a raft. One problem with this model is that it is extremely difficult to prove that the Clava Sand Member was frozen at the time of deformation.

3.2 THRUSTS AND HIGH STRAIN ZONES

The glaciofluvial ice-contact sands (Unit 4) exposed in Section III are deformed by a number of northeasterly dipping thrusts (Figure 3 and 5). These thrusts are marked by up to 50 cm thick zone of apparently highly deformed, stiff laminated clay, silt and sand (Figure 5). Lenses or boudins of fine- to medium-grained sand and pebbly diamicton also occur within these 'high-strain zones'. A number of the lenses of diamicton are lithologically similar to the structurally underlying Clava Shelly Till Member and have yielded shell fragments (Peacock, 1975). A thrust-bound wedge of the basal part of the Clava Sand Member occurs in the immediate hanging-wall of the thrust forming the base to the main part of the glaciofluvial unit (Figure 3). The apparently erosive contact between the glaciofluvial ice-contact deposits (Unit 4) and the underlying Clava Shelly Till and Clava Sand members is exposed in the central to north-northeastern end of the stream section (Figure 3).

At the south-southwestern end of Section III the sediments in the upper part of the Clava Sand Member, immediately below the tectonised base of Unit 4, possess a wavy lamination or foliation which Merritt (1992) interpreted as having developed due to subglacially induced ductile shearing. The Clava Sand and Clava Shelly Till members are deformed by open to tight, apparently southeasterly verging asymmetrical, northwesterly plunging folds which result in the localised overturning of bedding. The upper limb of one of these folds is cut by a sand-filled hydrofracture (Figure 3). The actual relationship of the hydrofracturing to the folding is unclear. However the hydrofracture is clearly cut by the bounding thrust at the base of Unit 4. In the centre of the stream section, bedding within the Clava Sand Member is deformed by a northeasterly verging monocline. The asymmetrical fold and monocline are truncated by the moderately (c. 40°) northwesterly dipping thrust at the base of Unit 4 (Figure 3), indicating that folding pre-dated thrusting. However, this does not necessarily mean that the folding and thrusting represent completely separate deformation events. The ice movement direction during both the folding and thrusting was towards the east-southeast (Merritt, 1992).

The Clava Sand Member at the base of the section is deformed by a number of small-scale, steeply dipping (50° - 60°), conjugate normal faults. These fault planes dip to both the north and south, and clearly off-set the earlier developed folds.

4 Micromorphology

Six samples (N4691; N4692; N4693; N4694; N4695; N4696) of the glaciogenic sediments were collected from Section III [NH 7637 4369] and ‘Main Pit’ [NH76583 44081] (Table 2). The samples were obtained using 10 cm square, aluminium kubiena tins which were either cut or pushed into the face of the exposure (Figures 4 and 5). Once the samples were removed from the exposed face they were double sealed in plastic bags and stored at 4°C to prevent drying out and bacterial alteration prior to sample preparation. Sample N4691 was taken from a prominent high strain zone deforming the glaciofluvial ice-contact sediments exposed Section III. Sample N4692 is of the Clava Shelly Till Member exposed at the base of this section. Samples N4693, N4694, N4695 and N4696 were collected from a major hydrofracture system present within the thinly bedded to laminated sands, silts and clays of the Clava Sand Member (Unit 3b) exposed in the ‘Main Pit’ section. The first three samples were collected at the same stratigraphic level so any lateral variations in the hydrofracture system and host sediments could be studied. Sample N4696, however, was collected from a structurally much higher position where the steeply dipping hydrofracture system cross-cut bedding within the Clava Sand Member associated with a zone of brecciation.

Table 2. Details of samples collected from Section III and the ‘Main Pit’ at Clava.

Sample Number	Location	Grid Reference	Description
N4691 (QX194)	Section III, stream section, west of Drummore of Clava	[NH 7637 4369]	deformed silt, sand and clay within ‘high-strain zone’ marking thrust near the base of Unit 4
N4692 (QX1950)	Section III, stream section, west of Drummore of Clava	[NH 7637 4369]	massive grey overconsolidated diamicton, Clava Shelly Till Member
N4693 (QX196)	Clava ‘Main Pit’	[NH76583 44081]	laminated sand, silt and clay cut by a clay lined hydrofracture, Clava Sand Member
N4694 (QX197)	Clava ‘Main Pit’	[NH76583 44081]	deformed laminated silt, clay and sand with microfaults and boudinaged silty sand layers, Clava Sand Member
N4695 (QX198)	Clava ‘Main Pit’	[NH76583 44081]	sand-filled hydrofracture cutting laminated sand, silt and clay, Clava Sand Member
N4696 (QX200)	Clava ‘Main Pit’	[NH76583 44081]	deformed laminated silt, sand and clay cut by a complex clay and sand-filled hydrofracture, Clava Sand Member

4.1 ANALYTICAL TECHNIQUES

A total of 6 large format thin sections were prepared by Mr D. Oates at the British Geological Survey’s Thin Sectioning Laboratory (Keyworth) following the procedures for sample preparation of unlithified or poorly lithified materials. The thin sections were examined using a standard Zeiss petrological microscope and Zeiss projector enabling the analysis of both large and small-scale microscopic textures and fabrics. An annotated scanned image (Figures 6 to 11) of each thin section has been used to describe the main microscopic features developed within these Quaternary deposits.

4.2 TERMINOLOGY

The description and interpretation of the micromorphology and deformation structures developed within glacial deposits is a relatively recent and still developing technique (see van der Meer 1987, 1993; Seret 1993; van der Meer *et al.*, 1990; van der Meer *et al.*, 1992; van der Meer and Vegers, 1994; Menzies, 2000). Although repetitive features have been recognised (see van der Meer, 1987, 1993 and references therein), a standard nomenclature has yet to be formalised. The terminology used in this report is that proposed by van der Meer (1987, 1993) and Menzies (2000), and is based upon nomenclature developed by pedologists (for references see van der Meer, 1993). A definition of the terms used for the various textures and fabrics, and their proposed mode of formation is given below.

Plasmic fabric - The arrangement of high birefringent, optically aligned clay plasma/domains which are visible under the microscope (under cross polars). These fabrics are only observed when the sediment is clayey. Sediments containing little fines or a relatively high proportion of carbonate within the matrix do not exhibit a well-developed plasmic fabric.

Unistrial plasmic fabric - A planar plasmic fabric defined by relatively continuous domains typically defining discrete shears. Interpreted as developing in response to planar movement (van der Meer, 1993).

Skelsepic plasmic fabric - A plasmic fabric in which the orientated domains occur parallel to the surface of large grains. Interpreted as developing in response to rotational movement (van der Meer, 1993).

Lattisepic plasmic fabric - A plasmic fabric defined by short orientated domains in two perpendicular directions. In many cases this fabric is found associated with a skelsepic plasmic fabric. Therefore, lattisepic plasmic fabrics are also interpreted as having developed in response to rotational movement (van der Meer, 1993).

Omnisepic plasmic fabric - A plasmic fabric in which all the domains have been reoriented. Interpreted as developing in response to rotational movement (van der Meer, 1993).

Till 'pebbles' - Formed by rotational movement (van der Meer, 1993). They are subdivided into three types: Type (1) consists of till which lack an internal plasmic fabric. They are defined by encircling voids and the shape of the 'pebbles' becomes progressively angular and flatter with depth; Type (2) is characterised by 'pebbles' of fine-grained material which were part of the original sediment host. They are recognised by an internal plasmic structure and are not defined by voids; Type (3) form isolated 'pebbles' of either till or fine-grained sediments and are usually interpreted as having formed by reworking of the till. They may or may not contain internal plasmic fabrics.

Other microscopic features - These include: the circular arrangement of clasts (skeleton grains) with or without a 'core stone', interpreted as having formed in response to rotation (van der Meer, 1993); pressure shadows which are also interpreted as having formed in response to rotation (van der Meer, 1993); dewatering structures associated with shearing; microboudinage; microscopic-scale primary sedimentary structures (e.g. lamination, cross-lamination....etc); water-escape structures associated with forceful dewatering; and crushing of clastic grains.

4.3 THIN SECTION DESCRIPTIONS

Collectors Number: QX194. **Registered Number:** N4691. **Location:** [NH 7637 4369] Section III, stream section west of Drummore of Clava, orientation of face 150°. **Lithology:** deformed, laminated sand, silt and clay from 'high-strain zone' near to the base of the glaciofluvial ice contact deposits (Unit 4).

Description: This thin section is of a deformed and disrupted laminated silt, sand and clay representing one of the 'high-strain zones' which deformed the glaciofluvial ice contact deposits (Unit 4). The sand and silt layers are graded (fining upwards) indicating that these sediments are, in general, the right way up. The sample is mainly composed of weakly laminated to massive sand with minor intercalations of silt and clay (Figure 6). The sand is fine- to medium-grained with an open, clast to matrix supported texture. The matrix, where present, is patchily developed and composed of fine silt and clay. Lenticles of matrix-supported sand locally occur within the clay-rich bands and laminae. Sand grains are angular, subangular to rarely subrounded in shape with a low to moderate sphericity. The clast assemblage is dominated by monocrystalline quartz and plagioclase. Other minor to accessory detrital components include polycrystalline quartz, metasandstone (psammite), granite, muscovite, tourmaline, amphibole, garnet, titanite, epidote, zircon, zoisite, biotite, opaque minerals, K-feldspar and apatite. The rock fragments tend to form the larger coarse sand, small granule to rare pebble-sized clasts (Udden 1914). The sedimentary lamination is distorted around these granule to pebble sized clasts. No obvious kinking of detrital micas or crushing of detrital grains have been recorded in this sample.

The clay-rich layers are composed of finely laminated fine silt and clay. The thicker laminae are graded from silt, at the base, to clay at the top. Thin lenticles of matrix-supported sand occur parallel to this lamination. The clay is highly birefringent and possesses a well-developed bedding-parallel plasmic fabric which is defined by optically aligned clay plasma. This bedding-parallel foliation is deformed by small-scale kink-like folds, shears and is locally distorted around included detrital sand grains; the latter possibly occurring in response to compaction/loading. The shears define an anastomosing set of thrusts which are preferentially developed within the clay layers (Figure 6). These thrusts occur at a low-angle to bedding and locally truncate the lamination. This lamination is also off-set by a number of low angle to moderately dipping normal and reverse faults (Figure 6). A number of these faults also deform the adjacent sand layers.

The inter-relationships between the clay-rich and sand-rich layers are locally complex, and indicate that the layering present within this sample is not simply sedimentary in origin. In the upper part of the thin section a thick unit of sand is cross cut by a narrow band of highly birefringent clay. This clay clearly cross-cuts the lamination within the sand and follows an earlier formed funnel-like sand-filled water-escape conduit. This conduit is terminated abruptly at the top of the sand layer and does not penetrate the overlying clay. The lamination in the sand comprises alternating layers of clean, matrix-poor, clast-supported sand and a red-brown, matrix-supported sand which contains a birefringent clay matrix. This matrix is petrographically similar to the adjacent clay-rich laminae. In the upper part of this sand unit the lamination is more diffuse and the sediment has a more mottled appearance, compatible with liquefaction and remobilisation of the sand. The upper and lower boundaries of the sand unit are sharp, but highly irregular to sutured in form and clearly cross-cut the lamination and deformation structures developed within the adjacent clay-rich units (Figure 6). Similar complex, irregular, cross-cutting relationships are apparently along the boundaries of other sand layers within this sample. In some of these layers, the individual sand laminae are reverse graded (coarsening upwards) and may be cross-cut by small, clay lined water-escape conduits. Importantly, the majority of the sand layers do not show any evidence of the thrusting/shearing within the adjacent clay-rich layers.

In the lower part of the thin section the relationships between the sand- and clay-rich components of the sample are even more complex. The clay-rich layers vary in width across the thin section. The thickest of these is cut by an anastomosing network of faults or shears and contains augen-shaped lenses and lenticles of matrix-supported sand, which locally cross-cut the lamination in the adjacent silt and clay. The matrix-supported texture of the sand lenticles suggests that the clay matrix was introduced whilst the sand was in a highly dilated state. The overlying sand-dominated unit is highly disrupted and contains ribbons and angular fragments of laminated to massive silt and clay. The diffuse nature of the lamination and crosscutting relationships

displayed by the sand suggests that it has undergone varying degrees of liquefaction and remobilisation. In the central part of the thin section, this sandy unit is cross cut by a tree-like, branching clay-filled water-escape conduit (Figure 6). The fill in the upper part of the water-escape conduit is composed almost entirely of highly birefringent red-brown clay which is petrographically similar to a clay cutan. At its base, however, the fill grades from a pale grey silty clay into pale brown clay, forming a geopetal-like basal 'lag' to this complex water-escape feature.

Projections from the sand unit at the base of the thin section fill a complex vein which cross-cuts the overlying clay. In the right hand corner of the thin section, this sand layer is truncated by a moderately dipping fault which has formed the focus for a later water-escape conduit and associated disharmonic folding (Figure 6).

The cross-cutting relationships and irregular boundaries displayed by the sand-rich layers within sample N4691 have been interpreted as indicating the injection of this material along the lamination. The fluidisation and remobilisation of the sand is suggested by: the diffuse to locally complex nature of the lamination within these layers; disharmonic folding of the sand laminae; the presence of reverse grading; and the open packed, cement/matrix-supported texture of some sand laminae. The cross-cutting relationships between individual sand laminae suggests that liquefaction and remobilisation occurred several times. The apparent absence of deformation structures within the majority of the sand layers, in comparison to the adjacent clay-rich layers, suggests that liquefaction and injection occurred during the later stages or after deformation had ceased. It is possible that initial deformation of these laminated sediments was initially partitioned into the clay-rich layers leading to thrusting and minor repetition of these fine-grained sediments. However, as deformation continued the increase in load formed by the stacking of the Quaternary glaciogenic sequence and/or as a result of the overriding ice resulted in an increase in pore water pressure. This would have led to the liquefaction and remobilisation of the sand layers with any imposed shear being transmitted through these relatively weak, water-rich detachments.

Collectors Number: QX195. **Registered Number:** N4692. **Location:** [NH 7637 4369] Section III, stream section west of Drummore of Clava, orientation of face 163°. **Lithology:** massive, grey-green diamicton, Clava Shelly Till Member (Unit 3a).

Description: This thin section is of a fine-grained, matrix-supported, compact, massive diamicton containing well-dispersed granule to small pebble-sized (Udden 1914) lithic clasts (Figure 7). The matrix, where present, is patchily developed and composed of fine silt to clay-grade material. Lenticles of matrix-supported sand locally occur within the clay-rich bands and laminae. Detrital grains are angular to subangular in shape with a low sphericity. They are mainly composed of monocrystalline quartz, plagioclase and metamorphic and granitic rock fragments. Other detrital components include polycrystalline quartz, amphibole, biotite, muscovite, garnet, opaque minerals, zircon and chlorite. Rare shell fragments (?gastropod) are also present. Sparse till pebbles are also noted within this sample. The larger clasts are enclosed within a finer grained envelope or coating of clay which locally possesses a well-developed skelsepic plasmic fabric. The detrital micas are shape aligned parallel to a variably developed plasmic fabric present within the matrix of the diamicton.

The matrix to the diamicton is green-brown to yellow-brown in colour and composed of a very fine silty clay. The clay plasma are optically aligned and define two variably developed plasmic fabrics: (i) the first occurs parallel to the margins of the Clava Shelly Till Member; and (ii) a second more weakly/patchily developed, steeply inclined fabric which occurs parallel to a number of narrow, subvertical shears recognised along the right-hand-side of the thin section (Figure 7). These shears are diffuse with poorly defined margins and post-date the main foliation

within the matrix of the diamicton. There is no obvious preferred shape-alignment of detrital grains parallel to either of the plasmic fabrics present within the matrix. Local circular to arcuate grain arrangements can occur locally. These include turbate or crude galaxy textures developed around larger granule to pebble sized clasts.

Collectors Number: QX196. **Registered Number:** N4693. **Location:** [NH 76583 44081] Clava 'Main Pit', orientation of face 036°. **Lithology:** laminated sand, silt and clay cut by a clay-lined hydrofracture, Clava Sand Member (Unit 3b).

Description: This thin section is of variably deformed, laminated sand, silt and clay which is cross-cut by a steeply dipping, clay- and silt-filled hydrofracture (Figure 8).

The sand laminae or layers are composed of fine- to coarse-grained, locally pebbly, matrix-poor, open to very open packed, clast to locally matrix-supported, massive to weakly laminated sand. The sand laminae are locally reverse-graded (coarsening upwards). The margins of the sand layers are roughly parallel to the lamination in the adjacent silt and clay layers. However, although sharp, the margins of the sand layers are locally irregular to 'sutured' in form and cross-cut the lamination in these clay-rich units (Figure 8). Detrital grains within the sand-rich layers are angular, subangular to rarely subrounded. These clasts are mainly composed of monocrystalline quartz and subordinate plagioclase. Other minor to accessory detrital phases present include K-feldspar, biotite, epidote, muscovite, metasandstone (psammite), schistose semipelite, amphibole, garnet, tourmaline, zoisite, polycrystalline quartz, granite, mudstones, very fine-grained sandstone or siltstone, and clay cutan.

The clay-rich layers are composed of finely laminated fine silt and clay. The thicker laminae grade from silt, at the base, to clay at the top. Thin lenticles of matrix-supported sand occur parallel to, and locally cross-cutting this lamination. The clay is highly birefringent and possesses a well-developed bedding-parallel plasmic fabric, defined by optically aligned clay plasma. In some of the clay-rich layers, this bedding-parallel foliation is deformed by small-scale kink-like folds, shears and is locally distorted around included detrital sand grains; the latter possibly occurring in response to compaction/loading. The shears define an anastomosing set of thrusts, which are preferentially developed within the clay layers (Figure 8). These thrusts occur parallel to, or at a low-angle to bedding and locally truncate the lamination.

The laminated sand, silt and clay in the lower right-hand part of the thin section is cut by a prominent 20 to 30 mm across, sand, silt and clay-filled water-escape conduit. This broad water-escape feature dips at approximately 40° to 50° to the northeast. Cross-cutting relationships present within this feature suggest that it records several phases of liquefaction and water-escape. The earliest fill is composed of a patchy or mottled sand (F2 on Figure 8) with irregular, sutured contacts and diffuse internal lamination. This early sand-rich fill is cut by a later narrow band of laminated sand, silt and clay. The margins of this later feature are sharp and clearly cross cut the lamination within the first sand fill. This suggests that pore water pressure had fallen before the injection of the second phase fill, allowing the propagation of an open fracture through this originally liquefied sand. The second phase fill (LV1 on Figure 8) is laminated with individual laminae graded from fine, matrix-supported sand to silt and clay. The laminated nature of this fill indicates that several phases of fluid flow occurred along this structure. This laminated veinlet is, itself, cross-cut by a later vein composed of similarly laminated sand, silt and clay (LV2 on Figure 8).

In the upper, right-hand part of the thin section a funnel-shaped water-escape conduit is filled by a distinctive clay-fragment microbreccia (MB on Figure 8). This breccia-filled feature clearly cross-cuts the overlying layers and links into a layer-parallel band of breccia. This breccia layer is cut by the underlying reverse graded sand layer, indicating that brecciation and water-escape pre-dated the formation/injection of this reverse graded sand.

The most prominent feature present in sample N4693 is a steeply inclined hydrofracture which dips at approximately 70° to 80° southwest. The earliest fill within this hydrofracture is a breccia composed of angular, variably plastically deformed fragments of laminated clay and silt within a matrix of silty sand (HF1 on Figure 8). This fill is only preserved in the upper part of the hydrofracture (see Figure 8). The main fill comprises a complex vein-like network of sand containing irregular patches or fragments of laminated, highly birefringent clay (HF2 on Figure 8). The final fill is composed of a red-brown, weakly laminated, highly birefringent clay (HF3 on Figure 8).

The cross-cutting relationships and irregular boundaries displayed by the sand-rich layers within sample N4693 have been interpreted as indicating the injection of this material along the lamination. The fluidisation and remobilisation of the sand is suggested by: the diffuse to locally complex nature of the lamination within these layers; the presence of recognisable sand-filled water-escape conduits; the presence of reverse grading (not diagnostic); and the open packed, cement/matrix-supported texture of some sand laminae. The cross-cutting relationships between individual sand laminae suggests that liquefaction and remobilisation occurred several times. The apparent absence of deformation structures within the majority of the sand layers, in comparison to the adjacent clay-rich layers suggests that liquefaction and injection occurred during the later stages or after deformation had ceased. This is supported by the fact that the boundaries of one or two of the sand layers cross cut the earlier developed thrust faults and shears. Furthermore, fragments of birefringent clay which possesses a well-developed plasmic fabric occur within some sand layers. It is possible that initial deformation of these laminated sediments was initially partitioned into the clay-rich layers leading to thrusting. However, as deformation continued the increase in load formed by the glaciectonic stacking of the Quaternary glaciogenic sequence and/or as a result of the overriding ice resulted in an increase in pore water pressure. This would have led to the liquefaction and remobilisation of the sand layers with any imposed shear being transmitted through these relatively weak, water-rich detachments.

The originally layer-parallel injection of the fluidised sand was followed by the development of the cross-cutting, inclined water-escape conduits and hydrofractures. The result is a complex history of liquefaction, remobilisation and hydrofracturing which followed an initial phase of layer-parallel thrusting/shearing. The sequence of events recognised in sample N4693 can be summarised in the following stages:

Stage 1 – localised bedding-parallel thrusting/shearing that was apparently partitioned into the clay-rich horizons;

Stage 2 – liquefaction, remobilisation and injection of sand layer SS1 at a low-angle and cross cutting the sedimentary lamination (Figure 8);

Stage 3 – liquefaction, remobilisation and injection of sand layer SS2. This layer cross-cuts the sedimentary lamination in the underlying deformed clay and fills a sub-vertical water-escape conduit. This water-escape feature is truncated by an apparently later sand layer (SS4 on Figure 8);

Stage 4 – liquefaction, remobilisation and possible injection of highly irregular shaped layers of coarse-grained to pebbly sand CS1 (Figure 8). The relationship of this coarse-grained sand to the previously formed sand layers is unclear as no cross cutting relationships are apparent in this thin section;

Stage 5 – liquefaction, remobilisation and injection of weakly laminated sand layer SS3, which cross-cuts the underlying coarse sand CS1 (Figure 8);

Stage 6 – liquefaction, brecciation and injection of clay microbreccia (MB) and formation of funnel-shaped water-escape conduit cross-cutting the sedimentary lamination in the overlying clay-rich layer and earlier SS1 and SS2 sand layers (Figure 8). The cross-cutting relationship

indicates that pore water pressure was sufficient to lead to liquefaction of the host laminated, clay silt and sand;

Stage 7 – liquefaction, remobilisation and injection of laminated and reverse graded sand layer SS4 which cross-cuts the sedimentary lamination and thrust in the underlying deformed clay and overlying clay microbreccia (MB) (Figure 8);

Stage 8 – liquefaction, remobilisation and injection of sand layer SS5 which cross-cuts the clay microbreccia-filled water-escape conduit and earlier SS2 sand (Figure 8);

Stage 9 – liquefaction, remobilisation and injection of weakly laminated F2 sand into a relatively broad, moderately inclined water-escape conduit (Figure 8);

Stage 10 – fall in pore water pressure after injection of F2 sand, followed by hydrofracturing and introduction of laminated sand, silt and clay LV1 fill (Figure 8). Laminated and graded nature of fill suggests variation in flow regime and possibly multiphase fill to hydrofracture. The latter must have remained open for a prolonged period to allow repeated phases of fluid flow;

Stage 11 – hydrofracturing and deposition of LV2 laminated fill in vein-like fracture, which cross-cuts LV1 fracture fill, F2 sand and SS3 sand layers (Figure 8);

Stage 12 – hydrofracturing and formation of steeply dipping brittle fracture. Initial brecciated clay-fill (HF1) is only preserved in the upper part of the hydrofracture. Later phases of fluid flow along this open fracture resulted in the deposition of the complex HF2 and HF3 sand and clay fills (Figure 8).

Collectors Number: QX197. **Registered Number:** N4694. **Location:** [NH 76583 44081] Clava ‘Main Pit’, orientation of face 036°. **Lithology:** laminated sand, silt and clay with microfaults and boudinaged silty sand layers, Clava Sand Member (Unit 3b).

Description: This thin section is of variably deformed, laminated sand, silt and clay (Figure 9) and is lithologically similar to sample N4693. In this thin section (N4694), there is a marked contrast in the intensity of deformation recorded by the sands and laminated silts and clays. Deformation structures are preferentially developed within the laminated clay and silt layers. Layering within these layers is off-set by a number of small scale normal and reverse microfaults, and bedding-parallel shears and/or thrusts (Figure 9) The silt and clay-rich layers are locally highly birefringent and locally possess a well-developed layer-parallel plasmic fabric. This fabric is defined by optically aligned clay plasma. In some of the clay-rich layers, this bedding-parallel foliation is deformed by small-scale kink-like folds, shears and is locally distorted around included detrital sand grains; the latter possibly occurring in response to compaction/loading. Deformation within the sand layers is restricted to localised normal and reverse faulting within the central part of the thin section (Figure 9). Graded bedding within the sands, silt and clay layers indicate that they are the right-way-up and that deformation did not result in the overturning of these sediments.

The sand laminae or layers are composed of fine- to coarse-grained, locally pebbly, matrix-poor, open to very open packed, clast to locally matrix-supported, massive to weakly laminated sand. The sand laminae are locally reverse-graded. The margins of the sand layers are roughly parallel to the lamination in the adjacent silt and clay layers, However, although sharp, the margins of the sand layers are locally irregular, ‘sutured’ to locally flame-like in form and cross-cut the lamination in the clay-rich layers (Figure 9). Detrital grains within the sand-rich layers are angular, subangular to rarely subrounded in shape. These clasts are mainly monocrystalline quartz and subordinate plagioclase. Larger clasts are mainly composed of metamorphic (metasandstone (psammite), schistose semipelite) and granitic rock fragments. Other minor to accessory detrital phases present include polycrystalline quartz, muscovite, biotite, amphibole,

K-feldspar, siltstone, apatite, zircon, garnet, zoisite, granite and laminated clay and silt. Impersistent heavy mineral bands present in a number of the sand layers are dominated by angular fine sand-grade clasts of garnet and amphibole.

The clay-rich layers are composed of finely laminated fine silt and clay. The thicker laminae are graded from silt, at the base, to clay at the top (Figure 9).

The laminated sand, silt and clay in the upper part of the thin section is cut by a wide (20-30 mm across), sand, silt and clay-filled water-escape conduit (Figure 9). This broad water-escape feature dips at approximately 5° to 10° to the northeast. Cross-cutting relationships within this feature suggest that it records several phases of liquefaction and water-escape. The earliest fill is composed of a weakly laminated and normal (fining-upwards) and reverse (coarsening-upwards) graded sand with sharp, locally flame-like contacts (F2 on Figure 9). This early sand-rich fill is cut by a later narrow band of laminated silt (LV1 on Figure 9). The margins of this later feature vary from sharp to diffuse and clearly cross-cut the lamination within the first sand fill. The locally diffuse nature of the margins of this silt-filled veinlet suggests that the host sand still possessed a relatively high pore water content or pressure during the injection of the second phase fill, allowing partial liquefaction of the F2 sand immediately adjacent to the LV1 veinlet. The fill to the LV1 veinlet is graded from fine sand to silt (Figure 9) recording a change in flow regime during fluid flow. The F2 sand fill is also cut by a later weakly branching hydrofracture filled by a complex mixture of matrix-supported fine sand and highly birefringent clay (LV2 on Figure 9).

In the centre of the thin section a relatively thick sand layer is cut by an irregular veinlet filled by a distinctive clay-fragment microbreccia (MB on Figure 9). This breccia-filled feature is clearly terminated at the margin of the sand layer where it comes into contact with a laminated silty clay. The breccia is cut by an irregular layer or veinlet of coarse-grained sand (CS1 on Figure 9).

The most prominent deformation structures present in sample N4694 are a number of moderately to steeply inclined normal and reverse faults which off-set the lamination (Figure 9). Two sets of normal faults are recognised: the first set dips towards the northeast and either link into the layer-parallel thrust or are truncated by these structures; the second set are concentrated within the centre of the thin section and dip towards the southwest.

The cross-cutting relationships and irregular boundaries displayed by the sand-rich layers within sample N4694 is similar to N4693 and have been interpreted as indicating the injection of this material along the lamination. The range of structures associated with fluidisation and remobilisation of the sand are comparable to the previous samples and include: the diffuse to locally complex nature of the lamination within these layers; the presence of recognisable sand-filled water-escape conduits; the presence of reverse grading (not diagnostic); and the open packed, cement/matrix-supported texture of some sand laminae. The cross-cutting relationships between individual sand laminae suggests that liquefaction and remobilisation occurred several times. The apparent absence of deformation structures within the majority of the sand layers, in comparison to the adjacent clay-rich layers suggests that liquefaction and injection occurred during the later stages or after deformation had ceased. This interpretation is supported the earlier developed thrusts and shears are locally cross-cut by the fluidised sand layers. It is possible that deformation was initially partitioned into the clay-rich layers leading to thrusting. These layer-parallel structures would have represented planes of weakness and allowed fluidised sand to penetrate along bedding. Injection of the fluidised sand was followed by a fall in pore water pressure and/or content. Subsequent/continued deformation lead to normal and reverse faulting, and possible reactivation of earlier developed thrust faults.

The sequence of events recognised in sample N4694 can be summarised in the following stages:

Stage 1 – localised bedding-parallel thrusting/shearing which was apparently partitioned into the clay-rich horizons;

Stage 2 – liquefaction, remobilisation and injection of sand layer SS1 parallel to bedding (Figure 9);

Stage 3 – a fall in pore water pressure and/or content within the SS1 sand layer was followed by renewed thrusting and modification of the boundaries of this sand unit

Stage 4 – liquefaction, remobilisation and injection of SS2 and SS3 sand layers which cross-cuts the sedimentary lamination and thrusts developed in the adjacent clay and silt-rich layers and (Figure 9);

Stage 5 – a phase of extension resulted in normal faulting, layer-parallel attenuation and necking of the SS2 and SS3 sand layers. The normal faults off-set both the layering and the earlier developed layer-parallel thrusts (Figure 9);

Stage 6 – liquefaction, remobilisation and injection of the mud clast-rich microbreccia (MB on Figure 9);

Stage 7 – liquefaction, remobilisation and injection of weakly laminated sand layer SS4. Although cut by the normal faults this sand layer has not undergone the layer-parallel attenuation that affected SS2 and SS3 sands, indicating that injection of SS4 sand post-dated this phase of extension (Figure 9);

Stage 8 – liquefaction, remobilisation and injection of the coarse-grained sand layer (CS1 on Figure 9), which cross-cuts the SS4 sand and microbreccia (MB) layers;

Stage 9 – reactivation of earlier developed normal and reverse faults affecting the SS2 and SS3 sand layers. Displacement gradient noted along these faults with little off-set of the SS4, CS1 and MB layers (see Figure 9);

Stage 10 – liquefaction, brecciation and injection of SS5 sand layer. This sand locally possesses irregular, flame-like boundaries which cross-cut the sedimentary lamination and deformation structures developed within the adjacent clay and silt layers (Figure 9). The SS5 sand layer is unaffected by the faulting and layer-parallel attenuation;

Stage 11 – liquefaction, remobilisation and injection of weakly laminated and graded F2 sand (Figure 9). Relationship(s) of this sand filled water-escape conduit to the other sand layers present within sample N4694 is uncertain;

Stage 12 – hydrofracturing and injection of laminated silt (LV1 on Figure 9), cross-cuts the earlier developed F2 sand. The diffuse nature of the margins of this silt-filled veinlet indicate that the water content of the F2 sand was still high allowing the localised remobilisation of this earlier formed unit during the injection of the LV1 sediment fill;

Stage 13 – Hydrofracturing and injection of the clay, silt and sand (LV2 on Figure 9) filling a weakly branching water-escape structure. The outer part of the LV2 fill is composed of a highly dilated sand containing fragments of a highly birefringent clay cutan and clay cutan-like matrix or cement.

Collectors Number: QX198. **Registered Number:** N4695. **Location:** [NH 76583 44081] Clava 'Main Pit', orientation of face 034°. **Lithology:** laminated sand, silt and clay cut by a subvertical clay- and sand-filled hydrofracture, Clava Sand Member (Unit 3b).

Description: This thin section is composed of variably deformed, laminated sand, silt and clay which are cross-cut by a steeply dipping to subvertical, clay- and sand-filled hydrofracture (Figure 10). The overall range of lithologies in this thin section are similar to those present within the previously described samples (N4693, N4694) taken from the Clava 'Main Pit'.

The sand laminae or layers are composed of fine- to coarse-grained, matrix-poor, open to very open packed, clast to rarely matrix-supported, massive to weakly laminated sand. The sand laminae are locally reverse-graded and contain scattered granular to small pebble-sized clasts (Udden 1914). The margins of the sand layers are roughly parallel to the lamination in the adjacent silt and clay layers. Although typically sharp, the margins of the sand layers are locally irregular to 'sutured' in form and cross-cut the lamination in these clay-rich units (Figure 10). Detrital grains are angular, subangular to rarely subrounded in shape. These clasts are mainly composed of monocrystalline quartz and subordinate plagioclase. Other minor to accessory detrital phases present include silt, clay, biotite, muscovite, garnet, opaque minerals, titanite, amphibole, apatite, K-feldspar, granite and metasandstone (psammite). The sands are, in general, undeformed. However, a number of the sand layers are cut by small-scale, silt-filled water-escape conduits.

The clay-rich layers are composed of finely laminated fine silt and clay (Figure 10). The thicker laminae are graded from silt, at the base, to clay at the top. Thin lenticles of matrix-supported sand occur parallel to, and locally cross-cutting this lamination. The clay is highly birefringent and possesses a well-developed bedding-parallel plasmic fabric, defined by optically aligned clay plasma. In some clay-rich layers, the bedding-parallel foliation is deformed by small-scale kink-like folds and shears. This fabric is also locally distorted around included detrital sand grains, possibly as a result of subsequent loading/compaction. The shears define an anastomosing set of thrusts or detachments that are preferentially developed within the clay layers (Figure 10). These thrusts occur parallel to, or at a low-angle to bedding and locally truncate the lamination. Deformation also resulted in localised disharmonic folding and/or brecciation. Brecciation appears to have been accompanied by the development of small-scale, silt-filled water-escape conduits which locally disrupt the lamination within the silt and clay layers. In the more intensely disrupted layers, angular fragments of laminated silt and clay occur as randomly orientated rafts suspended within a patchy matrix of cement-supported sand and silt. It is possible that brecciation of the clay and silt laminae occurred as a result of the liquefaction and remobilisation of the sand. Disharmonic folding and brecciation of the clay and silt layers predates the injection of the more massive sand layers. These sands clearly cross-cut the brecciated clay layers (see Figure 10) and are unaffected by this earlier phase of brittle deformation.

The cross-cutting relationships and irregular boundaries displayed by the sand-rich layers within sample N4695 have been interpreted as indicating the injection of these coarser grained layers along the lamination. The interpretation that the sands were introduced by a process involving fluidisation and remobilisation is supported by: the diffuse to locally complex nature of the lamination within these sand layers; the presence of recognisable sand-filled water-escape conduits within the sands; the presence of reverse graded (not diagnostic) laminae; and the open packed, cement/matrix-supported texture of some sand layers. The cross-cutting relationships displayed between individual sand layers (see Figure 10) suggests that liquefaction and remobilisation occurred several times. The apparent absence of deformation structures within the majority of the sands, in comparison to the adjacent clay-rich layers, suggests that liquefaction and injection occurred during the later stages or after deformation had ceased. This is supported by the fact that the boundaries of some of the sand units clearly cross-cut the earlier developed deformation structures. As in the previously described in sample N4694, these relationships suggest that deformation was initially partitioned into the clay-rich layers. As deformation continued the increase in load formed by the glaciectonic stacking of the Quaternary glaciogenic sequence, and/or as a result of the overriding ice, may have resulted in an increase in pore water pressure and repeated phases of liquefaction and remobilisation of the interlayered sands.

The most prominent feature present in sample N4695 is a steeply inclined to subvertical hydrofracture. The earliest fill within this hydrofracture is a breccia composed of angular, variably plastically deformed fragments of laminated clay and silt within a matrix of silty sand (HF1 on Figure 10). This fill is only preserved in the lower part of the hydrofracture. The main

fill to the hydrofracture is composed of weakly laminated to massive sand (Figure 10). In the lower part of the hydrofracture, this sand fills a vein-like network cutting the earlier developed breccia-like fill (Figure 10). The sand filled part of the hydrofracture is linked to an apparently layer-parallel unit of matrix-poor sand (bottom left of Figure 10). To the left of the main sand-filled hydrofracture is a much narrower clay and silt-filled fracture (HF2 on Figure 10). The clay is red-brown, weakly laminated, highly birefringent and possesses a well-developed plasmic fabric, which occurs parallel to the margins of the structure. This relationship suggests that the plasmic fabric developed in response to the ‘plastering’ of the clay plasma to the margins of the open fracture during fluid flow.

Sample N4695 records complex history of liquefaction, remobilisation and hydrofracturing, which followed an initial phase of layer-parallel thrusting/shearing. The sequence of events recognised in this sample can be summarised in the following stages:

Stage 1 – bedding-parallel thrusting/shearing which was apparently partitioned into the clay-rich horizons (Figure 10);

Stage 2 – localised disharmonic folding and brecciation within the clay- and silt-rich layers with accompanying liquefaction of interlayered sands (Figure 10);

Stage 3 – liquefaction, remobilisation and injection of coarse-grained sand (CS1 on Figure 10);

Stage 4 – liquefaction, remobilisation and injection of sand layer SS4 which cross-cuts the earlier developed disharmonic folds and CS1 sand (Figure 10);

Stage 5 – fall in pore water pressure and/or content followed by continued or renewed layer-parallel thrusting. The reactivated thrusts cut the SS4 and CS1 sand units;

Stage 6 – liquefaction, remobilisation and possible injection of highly irregular shaped layers of coarse-grained to pebbly sand CS1 (Figure 8). The relationship of this coarse-grained sand to the previously formed sand layers is unclear as no cross cutting relationships are apparent;

Stage 7 – localised normal and reverse faulting effecting the laminated silts and clay, and earlier formed CS1 coarse sands. These microfaults also locally off-set the layer-parallel thrusts;

Stage 8 – liquefaction, remobilisation and injection of the massive weakly laminated sand layer SS1. This sand cross-cuts the lamination in the adjacent silts and appears to thin laterally (Figure 10);

Stage 9 – liquefaction, remobilisation and injection of massive SS6 sand;

Stage 10 – liquefaction, remobilisation and injection of weakly laminated and reverse graded sand layer SS3 which cross-cuts the sedimentary lamination in the silts and clays, and the earlier formed SS6 sand (Figure 10). In the central part of the thin section, small-scale water-escape conduits cross-cut the SS3 sand;

Stage 11 – minor reactivation of earlier developed normal faults which locally off-set the margin of the SS3 sand layer;

Stage 12 – liquefaction, remobilisation and injection of sand layer SS5. The relationship of this unit to the earlier formed sand layers is uncertain;

Stage 13 – hydrofracturing and development of HF2 laminate clay and silt fill. This predominantly clay-filled hydrofracture cuts all the earlier developed deformation structures and sand layers (SS5, SS3, SS1, CS1) (Figure 10). This hydrofracture also appears to follow the earlier developed normal faults and occurs along the hinge of a kink-like fold (see Figure 10), indicating that earlier developed deformation structures may have, at least in part, controlled the site of hydrofracture development;

Stage 14 – hydrofracturing and introduction of the breccia-like HF3 laminated clay, silt and sand, silt and clay fill into a steeply dipping to subvertical hydrofracture system. The curved

nature of the layering within this fill is consistent with the effect of upward ‘drag’ of sediment during fluid flow;

Stage 15 – hydrofracturing and introduction of sand (SS7) into the earlier formed hydrofracture system (Figure 10). This relationship indicates that, once formed, a hydrofracture may reactivate several times and control water-escape over time. The resultant hydrofracture system may record a multiphase history of fracturing, fluid escape and sediment fill.

Collectors Number: QX200. **Registered Number:** N4696. **Location:** [NH 76583 44081] Clava ‘Main Pit’, orientation of face 039°. **Lithology:** deformed laminated sand, silt and clay cut by a complex, subvertical clay- and sand-filled hydrofracture, Clava Sand Member (Unit 3b).

Description: This thin section is composed of variably deformed, laminated sand, silt and clay which are cross-cut by a complex, steeply dipping to subvertical, clay- and sand-filled hydrofracture (Figure 11). The overall range of lithologies in this thin section are similar to those present within the previously described samples taken from the Clava ‘Main Pit’. However, the intensity of deformation and complexity of the sediment fill associated with this hydrofracture are far greater than that seen in the other thin sections (compare Figure 11 with Figures 8, 9 and 10).

The sand laminae or layers are composed of massive to weakly laminated, matrix-poor, open to very open packed, clast to rarely matrix-supported, fine- to coarse-grained sand. These laminae are locally reverse-graded and may contain scattered granular to small pebble-sized (Udden 1914) clasts (Figure 11). The margins of the sand layers are roughly parallel to the lamination in the adjacent silt and clay layers. Although sharp, the margins of the sand layers are locally irregular to ‘sutured’ in form and cross-cut the lamination in the clay-rich units. However, much of the sand present in sample N4696 has been introduced along the broadly funnel-shaped water-escape conduit which dominates this thin section (see Figure 11). Detrital grains within the sands are angular, subangular to rarely subrounded and mainly composed of monocrystalline quartz and subordinate plagioclase. Other minor to accessory detrital clasts include amphibole, opaque minerals, myrmekite, polycrystalline quartz, muscovite, biotite, epidote, titanite, garnet, K-feldspar, zoisite, apatite, granite, silt/siltstone, metasandstone (psammite) and metamafite rock fragments.

The clay-rich layers are composed of highly disrupted, finely laminated fine silt and clay (Figure 11). The thicker laminae are graded from silt, at the base, to clay at the top. Thin lenticles of matrix-supported sand occur parallel to, and locally cross-cutting this lamination. The clay is highly birefringent and possesses a well-developed bedding-parallel plasmic fabric, defined by optically aligned clay plasma. In some clay-rich layers, the bedding-parallel foliation is deformed by small-scale recumbent folds, kink-like structures and shears. Much of the early deformation structures, however, have been disrupted/overprinted by subsequent brecciation and the injection of fluidised sediment along the water-escape conduit.

As previously mentioned, the most prominent feature present within sample N4696 is a steeply inclined, funnel-shaped water-escape conduit which dips steeply towards the northeast (Figure 11). In detail this complex, multiphase feature is associated with a complex network of hydrofractures which result in the fragmentation/brecciation of the sediments in the adjacent ‘wall-rock’. The cross-cutting relationships and irregular boundaries displayed by the various generations of sand-rich and clay-rich fills (see Figure 11) within this water-escape conduit allow a relative chronology of sediment deposition to be established. The earliest phase of fill appears to have accompanied the brecciation of the laminated clay and silt in the adjacent ‘wall-rock’. This brecciation resulted in the disruption of earlier developed deformation structures (folds and thrusts). Fractures associated with this brittle deformation event are filled by a poorly sorted, fine- to medium-grained sand (CS1 on Figure 11) with an open packed, matrix-supported

texture. The matrix is composed of fine silt to clay. The CS1 sand cross-cuts all the earlier developed folds and faults developed within the clay and silt. The distribution pattern shown by this coarse sand-fill suggests that this fluidised sediment 'fanned out', upwards from a central conduit. The latter has been overprinted/reused by subsequent generations of sediment fill. The pattern of CS1 sand-filled veins may have been controlled by the pattern of brecciation developed at the tip of the main hydrofracture system. In the upper part of the thin section (top left of Figure 11), the CS1 sand-fill and adjacent sediments in the 'wall-rock' are deformed by a number of steeply dipping (dip to southwest), small-scale normal faults. These faults downthrow towards the southwest towards the centre of the water-escape conduit. Faulting may have occurred in response to the inward collapse of the funnel-shaped water-escape conduit after this phase of fluid flow had ceased; partially due to instability caused by the brecciation associated with this hydrofracture and/or evacuation of the sediment originally filling the main conduit. However, there is no evidence of any related faults on the opposite side of the water-escape conduit (see Figure 11). However, there is an apparent off-set, downthrow to southeast (i.e. normal), of the layering within the sediments of the adjacent wall rock (see Figure 11). Consequently, it is possible that the water-escape preferentially occurred along this pre-existing fault. The reactivation of this fault may have resulted in the minor faulting recorded in CS1 sand-fill. If correct this would suggest a structural control on the location of water-escape conduits.

The central upper part of the water-escape conduit is occupied by a crudely wedge-shaped unit of weakly laminated, coarse- to fine-grained sand (CS2 on Figure 11). This sand is texturally and compositionally similar to the CS1 sand-fill, but clearly cross-cuts this earlier developed sediment fill. The lamination within the CS2 sand fill is subhorizontal and the unit shows an overall upward fining sequence. This horizontal lamination and normal grading suggests that there was a change in flow regime during deposition. Deposition of the CS2 sand fill was followed by the injection of the fan-shaped CS3 sand which is preserved in the upper right-hand part of the thin section (Figure 11). This sand-fill possesses a patchy looking 'lamination' of matrix-poor (CS3a) and matrix-rich (CS3b) sand. The matrix is composed of a red-brown, highly birefringent clay to silty clay and locally results in a very open, matrix-supported texture. The CS3 sand appears to have been fed by a narrow vein-like conduit (Figure 11) which linked the site of sand deposition to the main water-escape structure.

The next event recorded in sample N4696 was in injection of a wedge-shaped unit of sand labelled SS2 on Figure 11. This overall massive sand occurs within the hanging wall of the main water-escape conduit. The weakly preserved lamination present within this sand is deformed by a moderate to steeply inclined asymmetrical fold in which the lower, over-turned limb has largely been overprinted due to the liquefaction and remobilisation of the sand. It is likely that liquefaction occurred during the later stages of the same deformation event which was responsible for the folding. A diffuse lamination present in the hinge area of the fold is deformed by small-scale, disharmonic M to weakly Z-shaped parasitic folds. The apparent dip of the axial surface of the fold is parallel to that of the adjacent water-escape conduit.

The main part of the water-escape conduit is filled by a complex network of sand silt and clay labelled HF1, HF2 and HF3 on Figure 11. The sandy HF1 fill possesses a diffuse lamination which is deformed by a number of disrupted, disharmonic folds. The complexity of these folds suggests that they may have formed during the initial stages of liquefaction and remobilisation. The later HF2 and HF3 fills display a complex relationship suggesting that they may have been injected during the same period of fluid flow. However, the clay-rich HF3 fill does appear to locally cut and, therefore, post date HF1. Injection of the later sediment fills appears to have resulted in localised drag folding of the HF1 fill along the boundary between the two generations of sediment infill (see Figure 11). HF3 is composed of a red-brown, highly birefringent clay.

It is clear from the above description that sample N4696 records complex history of liquefaction, remobilisation and hydrofracturing which followed an initial phase of layer-parallel

thrusting/shearing. The sequence of events recognised in this sample can be summarised in the following stages:

Stage 1 – bedding-parallel thrusting, shearing and folding which was apparently partitioned into the clay-rich horizons (Figure 11);

Stage 2 – injection of the weakly laminated SS1 sand parallel to the lamination within the host sediments;

Stage 3 – folding followed by the liquefaction and remobilisation of the wedge-shaped SS2 sand unit. Liquefaction of this sand during deformation resulted in the overprinting of the overturned, lower limb of the main fold structure and disharmonic nature of parasitic minor folds in its hinge (Figure 11);

Stage 4 – brecciation of the laminated previously deformed silt and clay followed by the injection of the coarse-grained CS1 sand along the main water escape conduit and into the network of fractures formed in the brecciated areas (Figure 11);

Stage 5 – fall in pore water pressure and/or content followed by localised normal faulting of the CS1 sand due to sediment either collapse within the water-escape conduit, or in response to a more widespread phase of extension and faulting;

Stage 6 – liquefaction, remobilisation and injection of the coarse- to fine-grained, graded CS2 sand which cross-cuts the earlier developed CS1 sand fill and is unaffected by the normal faults. Normal grading within the CS2 sand unit records a change in the flow regime (decreasing flow) during deposition;

Stage 7 – liquefaction, remobilisation and injection of the clast- to matrix-supported CS3 sand which is fed by a narrow vein-like off-shoot from the main water-escape conduit (Figure 11). The relationship of CS3 to the possibly earlier CS2 sand fill is uncertain due to later phase of sediment fill obscuring the contact;

Stage 8 – liquefaction, remobilisation and injection of the laminated LF1 sand, silt and clay (Figure 11) which cross cuts the earlier SS1, CS1 and CS3 sand-rich fills. The relationship between LF1 and HF1, HF2, HF3 are uncertain as no cross-cutting/interference relationships were observed in this thin section;

Stage 9 – minor faulting affecting LF1;

Stage 10 – liquefaction, remobilisation and injection of the internally complex, weakly laminated HF1 sand-dominated fill which cross cuts CS2 and CS1 (Figure 11). A variably preserved lamination is folded by disrupted/fragmented disharmonic folds;

Stage 11 – liquefaction, remobilisation and injection of the HF2 and HF3 which form the sediment fills to the main water-escape conduit (Figure 11). The complex relationship displayed between these two fills suggests that they may have been injected during the same period of fluid flow. However, the clay-rich HF3 fill does appear to locally cut and, therefore, post date HF1. Both HF2 and HF3 cross-cut the earlier developed CS1, CS2, CS3 and HF1 sediment fills. Injection of the later sediment fills appears to have resulted in localised drag folding of the HF1 fill along the boundary between the two generations of sediment infill (see Figure 11);

Stage 12 – liquefaction, remobilisation and injection of irregular patches of SS7 sand.

5 Evidence of multiphase water-escape during deformation of the glaciogenic sediments at Clava

It is clear from the above description that liquefaction, remobilisation and injection of the sand, silt and, to a lesser extent, clay played an important role during the deformation of the glaciogenic sedimentary sequence exposed at Clava.

5.1 THRUSTS AND HIGH STRAIN ZONES

Merritt (1992) demonstrated that the glaciogenic sediments at Clava, in particular the glaciofluvial ice-contact sands (Unit 4), are cut by several, major northeasterly dipping thrusts (Figure 3). Thrusting and associated folding occurred in response to the movement of ice towards the east-southeast (Merritt, 1992) and led to the imbrication of the sedimentary sequence. Individual thrusts being marked by thick zones (≤ 50 cm) of apparently highly deformed, extremely hard, laminated clay, silt and sand. An orientated thin section (N4691) taken through a prominent thrust/high strain zone which forms the base to the main part of the glaciofluvial unit (Figure 3), however, has revealed that the intensity of deformation within these 'high strain zones' is much less than expected based upon macroscopic evidence. In thin section, this 'high-strain zone' is composed of massive to weakly laminated sand with minor intercalations of silt and clay (see Figure 6). Deformation appears to have been concentrated within the clay-rich layers which are deformed by essentially layer-parallel thrusts, as well as low-angle to moderately dipping normal and reverse faults. A well-developed bedding-parallel plasmic fabric within the clay laminae is deformed by small-scale kink-like folds and narrow ductile shears; the latter typically occurring adjacent to the thrusts. The thickest clay layers contain augen-shaped lenses and lenticles of matrix-supported sand. Graded bedding within the silty laminae show that these sediments are the right-way-up and there is little evidence of overturning during deformation.

In contrast to the clay-rich layers, the sand layers are essentially undeformed and show only localised evidence thrusting/shearing along their margins and minor off-set by moderately inclined normal and reverse faults. In many cases, the sandy layers possess irregular, sutured to flame-like boundaries which cross-cut the lamination and deformation structures in the adjacent clays. The lamination within the sand, where preserved, is typically diffuse and defined by the variation in the modal proportion of a red-brown clay matrix. This clay is petrographically similar to a clay cutan. The matrix-rich layers possess an open, matrix or 'cement' supported texture, suggesting that the clay was introduced whilst the sand was in a highly dilated state. Reverse grading is also common within some of the sand layers.

Further evidence for fluid flow along the 'high strain zones' is provided by the presence of clearly cross-cutting water-escape features, or hydrofractures, within sample N4691. In the upper part of the thin section, an irregular water-escape conduit possesses a complex fill of matrix-rich sand, cut by a narrow band of highly birefringent clay (Figure 6). These cross-cutting generations of fill indicate that the water-escape conduit was active for a prolonged period and accommodated several phases of fluid flow. The conduit is terminated abruptly at the top of a sand layer and does not penetrate the overlying clay. The latter may have formed an impenetrable barrier to the upward migration of water, with the fluidised sand and, on a later occasion, clay being forced to flow laterally along parallel to the layering within the 'high strain zone'. Similar cross-cutting, irregular to branching sand and/or clay filled water-escape features are present in the lower part of sample N4691 (see Figure 6).

Microtextural relationships within the 'high strain zones' suggest that the sand layers have undergone liquefaction and remobilisation during deformation leading to the overprinting of any

earlier formed thrusts or folds. The lateral migration of the fluidised sand would have resulted in the observed cross-cutting relationships. Changes in the flow regime during liquefaction may have resulted in both normal and reverse grading of the sand. The fluidised sand layers would have also represented major planes of weakness within the 'high strain zone'. The effect of this water-rich sediment would have been to reduce the shear strength of the sediment by increasing pore water pressures and concentrating displacement along the fluidised sand layers. Due to the dilated state of the sand the sediment would have behaved like a viscous fluid and flowed rather than deformed, leading to the observed lack of deformation within these layers. Importantly, the presence of these fluidised sand layers within the 'high strain zone' would have effectively 'switched off' deformation within the adjacent hanging wall and footwall. Any shear induced by the overriding ice would have been accommodated by movement along the fluidised zones rather than being transmitted into the adjacent sediments. Movement of water along the 'high strain zones' would have resulted in a fluctuation in pore water pressure leading to a stick-slip style of movement along the thrust. During periods of low pore water pressure displacement would have potentially decreased and accommodated by layer-parallel brittle thrusting.

5.2 HYDROFRACTURING AND LAYER-PARALLEL FLOW ZONES IN THE CLAVA SAND MEMBER

Samples N4693, N4694, N4695 and N4696 were collected from a major hydrofracture system present within the thinly bedded to laminated sands, silts and clays of the Clava Sand Member (Unit 3b) exposed in the 'Main Pit' at Clava. The first three samples were collected at the same stratigraphic level within the Clava Sand Member allowing a correlation to be made between these thin sections, enabling a detailed chronology of events to be erected (Table 3). The final sample (N4696), however, was collected from a structurally much higher position where the steeply dipping hydrofracture system cross-cut bedding within the Clava Sand Member and was associated with a more obvious zone of brecciation. In detail the sequence of events recorded by these four thin sections are highly complex (see Table 3). However, this complex history can be simplified into four main events:

- (1) early phase of layer-parallel thrusting with associated folding and ductile shearing;
- (2) the repeated injection of fluidised sediment parallel to bedding/layering with minor thrusting and/or faulting;
- (3) the development of a broad water-escape conduit which cross-cut earlier developed layering;
- (4) hydrofracturing and deposition of the associated sand, silt and clay fills.

5.2.1 Event 1 - layer-parallel thrusting and associated deformation

The main phase of thrusting, folding and ductile shearing within the Clava Sand Member appears to have occurred early in the deformation history and was preferentially partitioned into the clay and silt-rich layers. This deformation event has been recognised in all of the samples collected from the 'Main Pit' at Clava.

Deformation resulted in the development of a locally pervasive bedding-parallel plasmic fabric within the clays. This fabric is locally deformed by small-scale recumbent folds, kinks and shears. The latter locally define an anastomosing set of essentially layer-parallel thrusts which result in the localised repetition and imbrication of the clays and silts (see Figures 8, 9 and 10). The lamination within the clay-rich layers is locally off-set by at least one set of small-scale normal and reverse faults (e.g. in sample N4694; Figure 9). These microfaults locally link into,

as well as off-set the layer-parallel thrusts and may have initially developed as Reidel shears. In sample N4695, thrusting was accompanied by localised disharmonic folding and brecciation. The brecciated areas are also cut by small-scale, silt-filled water-escape conduits which locally disrupt the lamination within the silt and clay layers. Thin lenticles of matrix-supported sand occur both parallel to, and locally cross-cutting the lamination within the clay-rich horizons (N6493; N6495). These microtextural relationships can be used to demonstrate that even at an early stage in the deformation history of Clava Sand Member, the coarser grained sediments were undergoing localised liquefaction and remobilisation.

In sample N4696, the early deformation structures developed within the clay-rich layers are disrupted/overprinted due to subsequent brecciation associated with the development of the prominent hydrofracture system which dominates this thin section (see section 5.2.4).

5.2.2 Event 2 – repeated layer-parallel injection of fluidised sediment

In contrast to the clays and silts, the majority of the sand layers within the thin sections (N6493, N6494, N6495, N6496) from the Clava Sand Member are essentially undeformed. These layers are composed of matrix-poor, clean sand which possesses an open to very open packed, clast to locally matrix-supported texture. The sands vary from massive to weakly laminated, with a variably developed normal (fining upwards) or reverse (coarsening upwards) grading. The lamination can be ‘diffuse’ to ‘patchy’ in nature, defined by a slight variation in grain size and/or matrix content. The margins of the sand layers are typically sharp and range from irregular, to ‘sutured’, to occasionally flame-like, and are only locally modified by later thrusting (e.g. sample N4694). In general, however, the sand layers cross-cut the sedimentary lamination and earlier formed deformation structures present within the adjacent clays and silts (see Figures 8, 9, 10 and 11). In samples N4693, N4694 and N4695, cross-cutting relationships have been recognised between the different sand layers (Figures 9 and 10). Also some in samples, the sand layers are locally off-set by a number of moderately to steeply inclined normal and reverse faults.

In samples N4693 and N4694 (Figures 8 and 9) the sands are cut by veinlets of a distinctive microbreccia (labelled MB) composed of angular clay fragments in a silty to sandy matrix. This microbreccia also fills a locally developed funnel-shaped water-escape conduit (Figure 8). The clay fragments are derived from the finely laminated clays within the Clava Sand Member.

The microtextural features displayed by the sand layers within the Clava Sand Member (including the cross-cutting relationships between sand layers; diffuse to locally complex laminations within the sands; the presence of recognisable sand-filled water-escape conduits; reverse grading; and the open packed, cement/matrix-supported texture) are consistent with the them having undergone varying degrees of liquefaction and remobilisation. This process overprinted any earlier developed deformation structures within the sands. Once remobilised, the fluidised sand injected along the lamination and possibly along earlier formed layer-parallel thrusts. These layer-parallel deformation structures would have represented planes of weakness, allowing fluidised sand to penetrate along bedding. However, pre-existing faults may have locally controlled fluid flow allowing the fluidised sand to transgress across the lamination. Individual phases of fluidised sand injection appears to have been followed by a fall in pore water pressure and/or content. This allowed the localised reactivation of earlier developed thrusts and minor normal and reverse faulting of the earlier formed sand layers.

Fluidisation of the sand is thought to have occurred in response to loading by the overriding glacier ice, with pore water pressure increasing as subglacial deformation continued. However, pore water pressure and/or content clearly fluctuated, leading to the repeated or episodic injection of sand along, possibly discrete, ‘flow zones’ within the Clava Sand Member. The fall in pore water pressure would have allowed shear to be transmitted into the sands resulting in the localised renewal of layer-parallel thrusting and/or related normal/reverse faulting. The

predominantly layer-parallel nature of the injection of the fluidised sand within the ‘flow zones’ can be used to suggest that either: **(i)** pore water pressure was insufficient to exceed the strength of the host sediments and the fluidised sand was ‘forced’ to utilise pre-existing planes of weakness such as bedding and/or bedding-parallel thrusts and shears; or **(ii)** the confining pressure of the overriding ice was sufficient to retard the formation of cross-cutting hydrofractures more typical of pressurised water-escape in less ‘confined’ systems; or **(iii)** a combination of these.

The volume of fluidised sand within the ‘flow zones’ (locally forming 60% to 70% of the thin section) clearly indicates that this process would have led to an increase in volume of the sediment. This volume change would have resulted in an expansion in the thickness of the sediment pile, requiring a decrease in the load exerted by the overriding ice. It is possible that pressure gradients existed below the glacier, for example associated with the margins of the glacier, or perturbations in the glacier bed such as bedrock highs. Liquefaction would have occurred in the relatively ‘high pressure domains’, hence leading to the removal of sediment (volume decrease) and sand deposition (volume increase) in the ‘low pressure domains’. The overall effect would have been one of pressure/deformation induced sediment transport.

5.2.3 Event 3 – development of the sand-filled water-escape conduit

In samples N4693 and N4694 the layer-parallel injection of fluidised sand (Event 2) was followed or accompanied by the formation of a cross-cutting water-escape conduit (Event 3) which channelled the flow of fluidised sand, silt and clay (see Table 3). The water-escape conduit (20 to 30 mm across) is internally complex, with several phases of fill having been recognised (Table 3). The earliest, and volumetrically most significant, fill is composed of a weakly laminated to massive sand (F2 on Figures 8 and 9). This early sand-rich fill is cut by a later narrow band of laminated sand, silt and clay (LV1). The margins of this laminated fill are sharp. This suggests that the pore water pressure/content in the F2 sand had fallen before the injection of the LV1 vein fill, allowing the propagation of an open fracture through the originally liquefied F2 sand. In sample N4694, however, the margins of the LV1 fill vary from sharp to diffuse. The LV1 fill is cross-cut by a later sediment filled (LV2) hydrofracture composed of laminated sand, silt and clay (Figures 8 and 9; also see Table 3).

The grading of the individual LV1 laminae indicates that the flow regime fluctuated during deposition. This, coupled with the laminated nature of the fill, suggests that once formed the hydrofracture (or veinlet) remained open for a prolonged period, enabling several phases of fluid flow to be channelled along this structure. It is possible that the plastering of clay plasma along the vein walls, indicated by the well-developed plasmic fabric within the LV1 clay, aided in the stabilisation the initial hydrofracture. However, the locally diffuse nature of the vein margins (see Figure 9) suggests that locally the F2 fill still possessed ‘patches’ with a relatively high pore water content. Flow of pressurised pore water along the fracture may have led to the partial liquefaction of the ‘moist patches’ within the F2 sand, and the localised destabilisation of the wall of the hydrofracture.

Event 3 recognised within the glaciogenic sequence at Clava ‘Main Pit’ is characterised by the development of cross-cutting water-escape conduits and hydrofractures during, rather than general fluid flow being essentially layer parallel as in Event 2. This change in morphology of the features associated with liquefaction and water-escape suggests that there may have been an overall increase in pore water pressure which exceeded the strength of the host sediments and/or confining pressure of the overlying ice leading to hydrofracturing of the Clava Sand Member.

5.2.4 Event 4 – main phase of hydrofracturing

The most prominent structures developed in samples N4693, N4695 and N4696 are a set of steeply inclined hydrofractures which cross-cut all the deformation and fluidisation/water-escape features developed during events 1, 2 and 3 (see Figures 8, 10 and 11, and Table 3). Rather than being simple structures, these hydrofractures comprise a complex sequence of fills recording a prolonged, multiphase history of fluid flow (Table 3). The most complex sequence of fills is recorded in sample N4696 (Figure 11 and Table 3), which occurs at a structurally higher position within the Clava Sand Member (see Figure 4). Sample N4695 occurs at a lower level within the same hydrofracture system, where it is considerably narrower and the associated brecciation of the ‘wall-rock’ is less intense (compare Figures 10 and 11). Sample N4693 is of a much narrower, apparently separate hydrofracture. However, it shows a similar cross-cutting relationship to all the features developed during the earlier events, and contains a series of fills which are lithologically similar to those present within the much larger hydrofracture system. Consequently, a tentative correlation can be made between these two brittle structures (see Table 3). The presence of a variably developed lamination and grading within some of the hydrofracture fills is thought to record changes in the flow regime during deposition. Normal (fining upwards) and reverse (coarsening upwards) grading demonstrate that the rate of fluid flow either decreased or increased, respectively during a single flow event.

The large, subvertical to steeply northeasterly dipping hydrofracture system has a narrow funnel-shape, widening upwards where it is associated with the a zone of brecciation (Figure 11). The earliest phases of fill (CS1, CS2, CS3; Figure 11) are only preserved within the upper part of the system (N4696), where they either form a network of vein-like, coarse sand fills (CS1) or fan-like fills (CS3) that emanated from narrow ‘veinlets’ fed by the main hydrofracture (Figure 12). These early fills are apparently absent in the lower part of the hydrofracture system (N4695) (Figure 10 and Table 3) either due to the lack of sediment deposition in this part of the fracture, or, alternatively the removal of these volumetrically small, sandy fills during later flow events. Small amounts of an earlier fill may be washed/eroded out of the main conduit during a later phase of peak fluid flow. The earliest fill (CS1) and adjacent ‘wall-rock’ sediments are deformed by a number of steeply dipping, small-scale normal faults. The downthrow of these faults towards the centre of the main hydrofracture system may be used to suggest that faulting occurred in response to the inward collapse of the funnel-shaped conduit after fluid flow had ceased. This may have occurred in response to instability caused by the brecciation of the adjacent wall-rock sediments and/or evacuation of the sediment originally filling the main conduit.

The main part of the hydrofracture system is filled by a complex system of sand, silt and clay fills (HF1, HF2 and HF3; Figure 11). These have been recognised in both sample N4695 and N4696 and appear to represent the a major phase of fluid flow and sediment deposition within the hydrofracture system. The presence of clay within these fills may have helped stabilise the walls of the hydrofracture. The plastering of clay plasma, indicated by the presence of a well-developed plasmic fabric within the clays parallel to the margins of the fracture, could have armoured the adjacent sediments, impeding fluid flow into and erosion of the adjacent sands, as well as effectively ‘cementing’ the fracture walls. A diffuse lamination within the earlier of sandy fills (HF1 and HF2) is deformed and disrupted by a number of disharmonic folds and is locally deflected upwards in response to drag folding associated with fluid flow upward through the hydrofracture. The complex interrelationships between the HF1, HF2 and HF3 suggesting that they may have been injected during the same overall flow event. However, the later clay-rich fill (HF3) locally cross-cuts the earlier sandy clay fills and was probably deposited during the waning stages of the flow event when only clay was transported. A similar chronology of lithologically similar sandy and clay-rich fills are recognised in sample N4693 (labelled HF1, HF2 and F3 on Figures 6 and 11).

The final flow event along the main hydrofracture system in samples N4695 and N4696 resulted in the deposition of a massive to very weakly laminated, matrix-poor sand (SS7). This clean sand cuts across the earlier fills and forms the dominant fill in the lower part of the hydrofracture system (Figure 10). At a higher level (N4696), flow appears to have been concentrated into a number of irregular fractures leading to the deposition of sand in a number of irregular pockets and veinlets (Figures 11).

As clear from the above, Event 4 within the glaciogenic sequence at Clava 'Main Pit' is characterised by hydrofracturing and multiphase fluid flow along these structures. These structures clearly developed in response to brittle deformation associated with the escape of pressurised pore water and fluidised sediment. The pressure of the escaping water-sediment mix exceeded the strength of the host sediments and/or confining pressure of the overlying ice leading to hydrofracturing of the Clava Sand Member. Once formed the hydrofractures formed a weakness within the glacier bed and became the focus for subsequent fracturing, accommodated several phases of water escape.

Table 3. Possible correlations between the various deformation, hydrofracturing and liquefaction events recognised in samples N4693, N4694, N4695 and N4696 collected from the 'Main Pit' at Clava.

	Sample Number			
	N4693	N4694	N4695	N4696
Event 1 - main phase of layer-parallel thrusting				
Stage 1	bedding-parallel thrusting/shearing partitioned into clay-rich horizons	bedding-parallel thrusting/shearing partitioned into clay-rich horizons	bedding-parallel thrusting/shearing partitioned into clay-rich horizons	bedding-parallel thrusting/shearing partitioned into clay-rich horizons
Stage 2			disharmonic folding and brecciation in clay-silt layers and liquefaction of intercalated sand laminae	
Event 2 - repeated injection of fluidised sediment parallel to layering with minor thrusting/faulting				
Stage 3	injection of SS1 sand parallel to layering	injection of SS1 sand parallel to layering	injection of coarse CS1 sand	injection of weakly laminated SS1 sand parallel to layering
Stage 4			injection of SS4 sand	
Stage 5		renewed layer-parallel thrusting and modification of the margins of SS1 sand	renewed layer-parallel thrusting	
Stage 6	injection of SS2 sand cross-cutting bedding and fills a sub-vertical water-escape conduit	injection of SS2 cross-cutting bedding		
Stage 7	injection of highly irregular shaped layers of coarse CS1 sand		injection of coarse CS1 sand	
Stage 8	injection of weakly laminated SS3 sand which pinches out laterally	injection of SS3 cross-cutting bedding		
Stage 9		normal faulting and boudinage of SS2 and SS3 sand layers	localised normal and reverse faulting	
Stage 10	injection of clay microbreccia (MB) and formation of funnel-shaped water-escape conduit	injection of clay microbreccia (MB)		
Stage 11	injection of laminated and reverse graded SS4 cross-cutting bedding	injection of weakly laminated SS4 sand cross cutting bedding	injection of the massive weakly laminated SS1 sand cross-cutting bedding	
Stage 12	injection of SS5 sand	injection of the coarse CS1 sand	injection of massive SS6 sand	
Stage 13		reactivation of earlier developed normal and reverse faults	injection of weakly laminated and reverse graded SS3 sand cross-cutting bedding	
Stage 14		injection of SS5 sand cross-cutting bedding	minor reactivation of normal faults	

Stage 15			injection of SS5 sand	
Event 3 - formation of broad, cross-cutting water-escape conduit				
Stage 16	formation of broad, moderately inclined water-escape conduit and injection of weakly laminated F2 sand	formation of broad, shallowly inclined water-escape conduit and injection of weakly laminated and graded F2 sand		?disharmonic folding and liquefaction of SS2 sand
Stage 17	hydrofracturing within Stage 9 water-escape conduit and deposition of laminated LV1 fill	hydrofracturing within Stage 12 water-escape conduit and deposition of laminated LV1 fill		
Stage 18	hydrofracturing within Stage 9 water-escape conduit and deposition of laminated LV2 fill	hydrofracturing within Stage 12 water-escape conduit and deposition of laminated LV2 fill		
Event 4 – main phase of hydrofracturing				
Stage 19	hydrofracturing, steep brittle fracture and formation of HF1 breccia fill			brecciation and injection of coarse CS1 sand into breccia along the main water-escape conduit
Stage 20				normal faulting of CS1 sand ?sediment collapse within the water-escape conduit
Stage 21				injection of graded CS2 sand
Stage 22				injection of the clast-to matrix-supported CS3 sand fed by a narrow off-shoot of main water-escape conduit
Stage 23				hydrofracturing, deposition of laminated LF1 fill
Stage 24				minor faulting of LF1
Stage 25			hydrofracturing, steep brittle fracture with internally complex HF2 sandy fill	injection of the internally complex HF1 sandy fill into water-escape conduit
Stage 26	injection of internally complex HF2 sandy fill into water-escape conduit			injection of sandy HF2 fill into the main water-escape conduit
Stage 27	deposition of clay-rich HF3 fill into water-escape conduit		hydrofracturing, steep brittle fracture and development of HF3 laminate clay-rich fill	deposition of clay-rich HF3 fills into the main water-escape conduit
Stage 28			injection of SS7 sand into main hydrofracture system	injection of SS7 sand into main hydrofracture system

Glossary

Micromorphology – A term used to describe the study of unlithified glacial sediments in thin section using a petrological microscope.

Plasmic fabric – The optical arrangement of high birefringent clay plasma/domains which are visible under crossed polarised light using a petrological microscope.

Unistrial plasmic fabric – A planar plasmic fabric defined by relatively continuous domains which is typically observed defining discrete shears (van der Meer, 1993).

Skelsepic plasmic fabric – A plasmic fabric in which the orientated domains occur parallel to the surface of large grains (van der Meer, 1993).

Lattisepic plasmic fabric – A plasmic fabric defined by short orientated domains in two perpendicular directions (van der Meer, 1993).

Omnisepic plasmic fabric – A plasmic fabric in which all the domains have been reoriented (van der Meer, 1993).

Grain size – (a) clay < 0.0039 mm in size; (b) silt, 0.0039 to 0.0625 mm in size; (c) fine sand, 0.0625 to 0.25 mm in size; (d) medium sand, 0.25 to 0.5 mm in size; (e) coarse sand, 0.5 to 1.0 mm in size; (f) very coarse sand, 1.0 to 2.0 mm in size; (g) granules 2.0 to 4.0 mm in size; (h) pebbles 4.0 to 64 mm in size.

Rounded – Describes the smoothness of the surface of a grain. The terms well-rounded, rounded, subrounded, subangular, angular, very angular are used to describe the increasingly angular/irregular/rough nature of the surface of detrital grains.

Sphericity – Describes how closely a detrital grain approximates to a sphere. The terms low sphericity, moderate sphericity and high sphericity are used to describe how spherical (ball-like) the detrital grains are.

Sorting – Well sorted describes a deposit in which all the detrital grains are of approximately uniform size. In reality most fragmentary deposits contain a range of grain sizes and can be described as moderately sorted, poorly sorted or in extreme cases unsorted.

Packing – Describes, as the term suggests, how closely the individual detrital grains are packed together within a fragmentary deposit. The term closely packed is used where all the grains are in contact and there is very little obvious matrix or cement; moderately packed and open packed are used with an increase in the porosity, matrix and/or cement.

Clast-supported – Describes a fragmentary deposit where all the detrital grains are in contact.

Clay cutan – a modified texture, structure or fabric of a unconsolidated material (e.g. soil) caused by the concentration of optically aligned, highly birefringent clay plasma.

Matrix-supported – Describes a fragmentary deposit where the detrital grains are, to varying degrees, isolated/supported within a finer grained matrix.

Cement-supported – Describes a fragmentary deposit where the detrital grains are, to varying degrees, isolated/supported within the cement.

Cement – The material bonding the fragments of clastic sedimentary rocks together and which was precipitated between the grains after deposition.

Porosity – The volume of voids expressed as a percentage of the total volume of the sediment or sedimentary rock.

Matrix – Material, usually clay minerals or micas, forming a bonding substance to grains in a clastic sedimentary rock. The matrix material was deposited with the other grains or developed authogenically by diagenesis or slight metamorphism. Also used more generally for finer grained material in any rock in which large components are set.

Detritus – A general term for fragmentary material, such as gravel, sand, clay, worn from rock by disintegration. Detrital grains in clastic sediments or sedimentary rocks may be composed of single mineral grains (e.g. monocrystalline quartz, plagioclase), polycrystalline mineral grains (e.g. polycrystalline quartz) or lithic fragments including sedimentary, igneous and metamorphic rock fragments.

References

Most of the references listed below are held in the Library of the British Geological Survey at Keyworth, Nottingham. Copies of the references may be purchased from the Library subject to the current copyright legislation.

ALLEY, R.B. 1989. Water-pressure coupling of sliding and bed deformation. *Journal of Glaciology*. **35**, 108-139.

BENNETT, M. & GLASSER, N. 1995. Process, bar morphology, and sedimentary structures on braided outwash fans, northeast Gulf of Alaska. In JOPLING, A.V. & MCDONALD, B.C. (eds) *Glaciofluvial and Glaciolacustrine Sedimentation. Special Publication of the Society of Economic Palaeontologists and Mineralogists*. **23**, 193-222.

BOULTON, G.S. 1972. Modern Arctic glaciers as a depositional model for former ice-sheets. *Journal of the Geological Society of London*. **128**, 361-393.

BOULTON, G.S. 1996. The origin of till sequences by subglacial sediment deformation beneath mid-latitude ice sheets. *Annals of Glaciology*. **22**, 75-84.

BOULTON, G.S. & HINDMARSH, R.C.A. 1987. Sediment deformation beneath glaciers: rheology and geological consequences. *Journal of Geophysical Research*. **92**, 9059-9082.

CLARKE, P.U. 1987. Subglacial sediment dispersal and till composition. *Journal of Geology*. **95**, 265-287.

MENZIES, J. 2000. Micromorphological analyses of microfabrics and microstructures indicative of deformation processes in glacial sediments. In Maltman, A. J., Hubbard, B. & Hambrey, J. M. (eds) *Deformation of Glacial Materials*. Geological Society, London, Special Publication. **176**, 245-257.

MERRITT, J.W. 1992. The high-level marine shell-bearing deposits of Clava, Inverness-shire, and their origin as glacial rafts. *Quaternary Science Reviews*. **11**, 759-77.

MURRAY, T. & DOWDESWELL, J.A. 1992. Water through flow and the physical effects of deformation of sedimentary glacier beds. *Journal of Geophysical Research*. **97**, 8993-9002.

OSTRY, R.C. & DEANE, R.E. 1963. Microfabric analyses of till. *Geological Society of America Bulletin*. **74**, 165-168.

PASSCHIER, C.W. & TROUW, R.A.J. 1996. *Microtectonics*. Springer.

PHILLIPS, E.R., CLARK, G.C. & SMITH, D.I. 1993. Mineralogy, petrology and microfabric analysis of the Eilrig Shear Zone, Fort Augustus, Scotland. *Scottish Journal of Geology*. **29**, 143-158.

SERET, G. 1993. Microstructures in thin sections of several kinds of till. *Quaternary International*. **18**, 97-101.

UDDEN, J.A. 1914. Mechanical composition of clastic sediments. *Bulletin of the Geological Society of America*. **25**, 655-744.

VAN DER MEER, J.J.M. 1987. Micromorphology of glacial sediments as a tool in distinguishing genetic varieties of till. In *INQUA Till Symposium, Finland 1985*. KUJANSUU, R. & SAARNISTO, M (editors). Geological Survey of Finland, Special Paper **3**, 77-89.

VAN DER MEER, J.J.M. & LABAN, C. 1990. Micromorphology of some North Sea till samples, a pilot study. *Journal of Quaternary Science*. **5**, 95-101.

VAN DER MEER, J.J.M., RABASSA, J.O. & EVENSON, E.B. 1992. Micromorphological aspects of glaciolacustrine sediments in northern Patagonia, Argentina. *Journal of Quaternary Science*. **7**, 31-44.

VAN DER MEER, J.J.M. 1993. Microscopic evidence of subglacial deformation. *Quaternary Science Reviews*. **12**, 553-587.

VAN DER MEER, J.J. M. & VEGERS, A.L.L.M. 1994. The micromorphological character of the Ballycraheen Formation (Irish Sea Till): a first assessment. In WARREN & CROOT (eds.) *Formation and Deformation of Glacial Deposits*. Balkema, Rotterdam. 39-49.

VERNON, R.H. 1989. Porphyroblast-matrix microstructural relationships: recent approaches and problems. In DALY et al. (eds). *Evolution of metamorphic belts*. Geological Society of London Special Publication. **43**, 83-102.

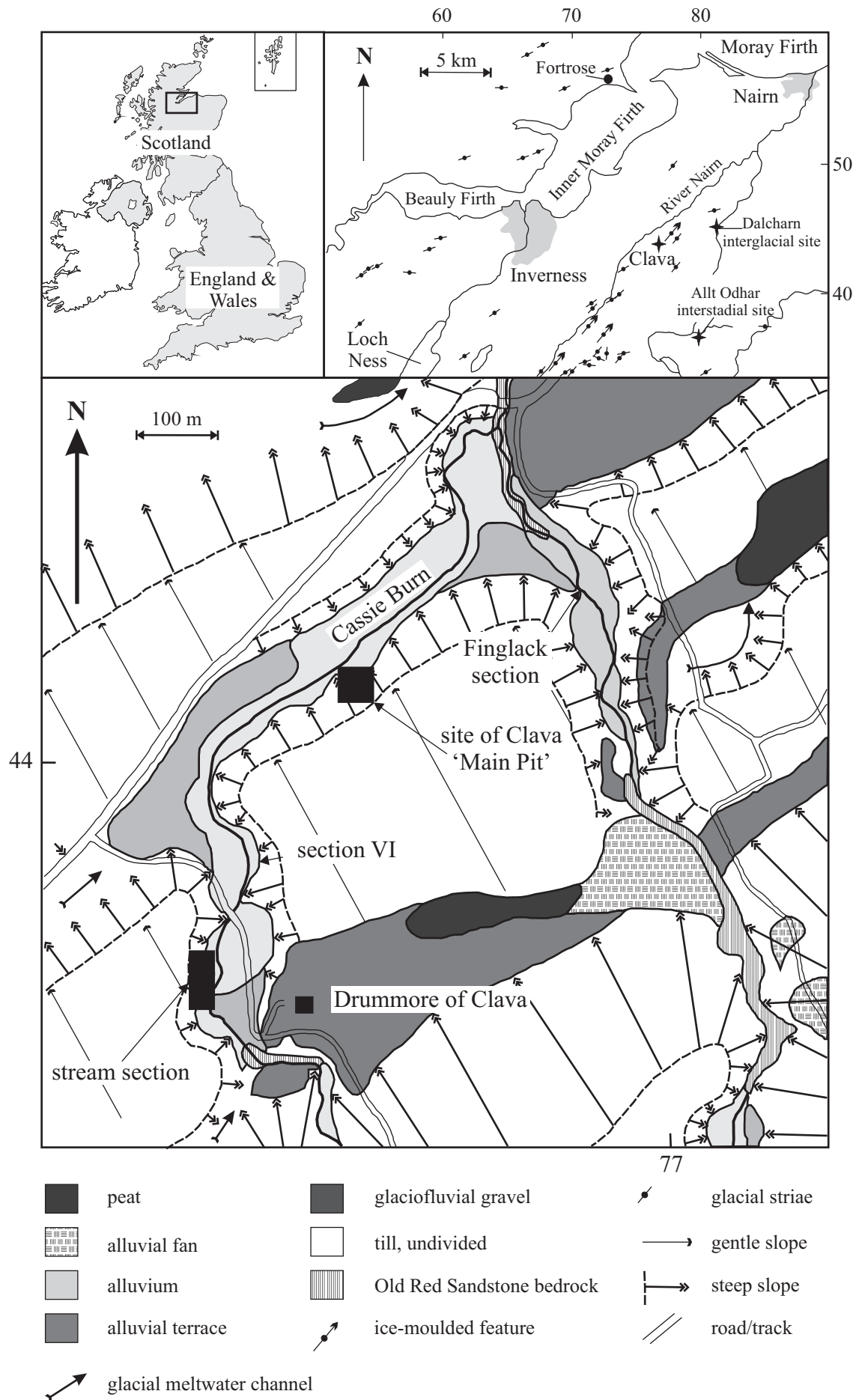


Figure 1. Simplified geological map of the Clava area showing the locations of the main sections studied (after Merritt, 1992). Insets - location maps.

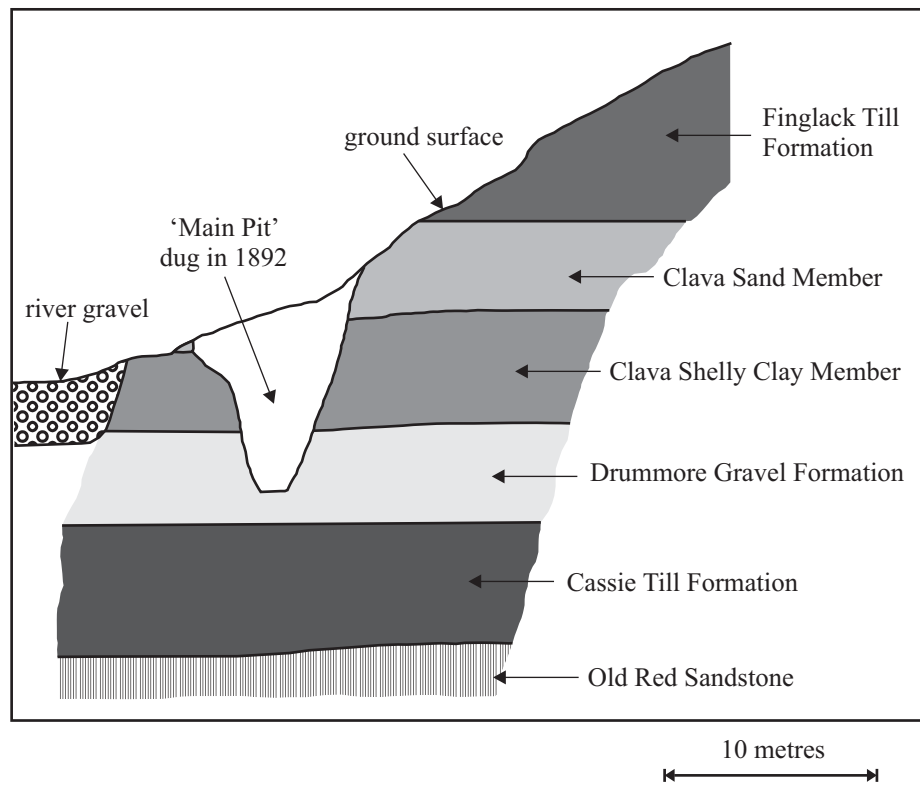


Figure 2. Section through the Pleistocene glacial sequence exposed in the 'Main Pit' (Merritt, 1992).

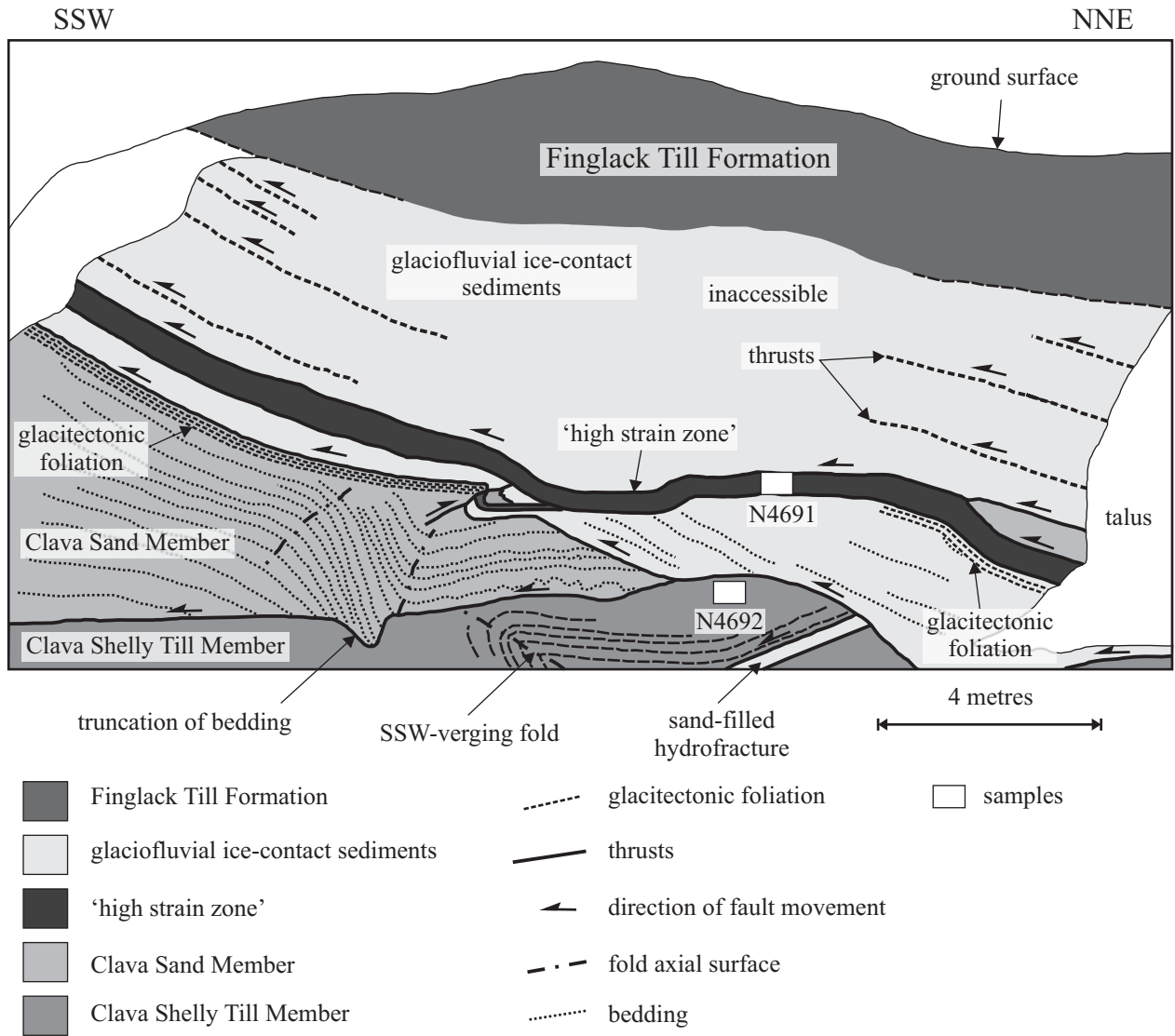
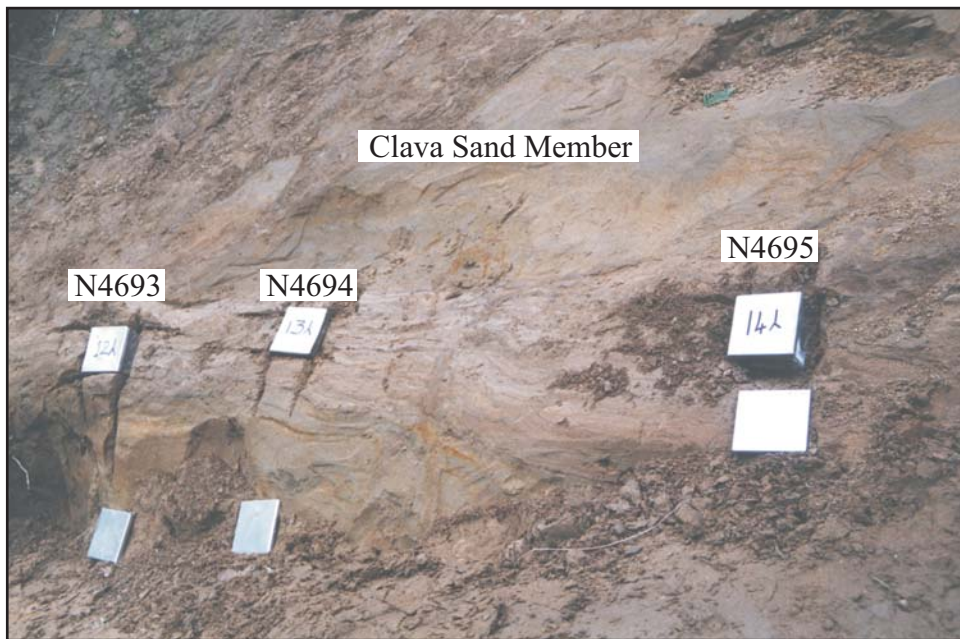
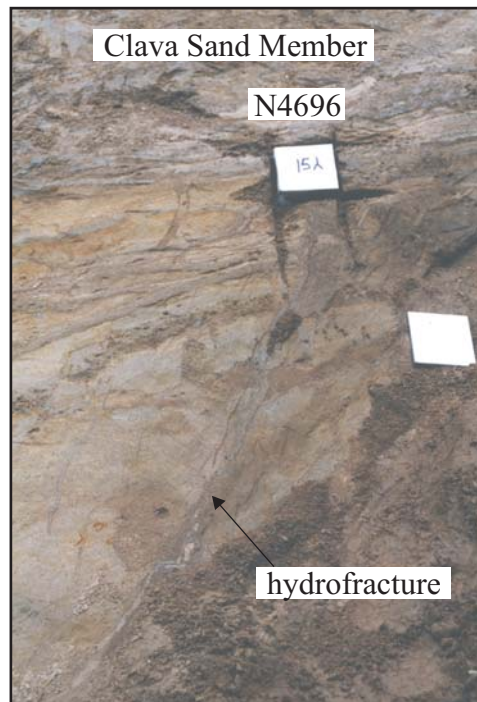


Figure 3. Section through the Pleistocene glacial sequence exposed in the stream section to the west of Drummore of Clava (Section III of Merritt, 1992). The approximate locations of samples N4691 (QX194) and N4692 (QX195) are also shown.



(a)



(b)

Figure 4. Photographs of laminated sand, silt and clay filled hydrofractures cutting the Clava Sand Member, the 'Main Pit' section. **(a)** subhorizontal hydrofracture showing location of samples N4693 (QX196), N4694 (QX197) and N4695 (QX198); **(b)** steeply dipping hydrofracture showing location of sample N4696 (Qx200).

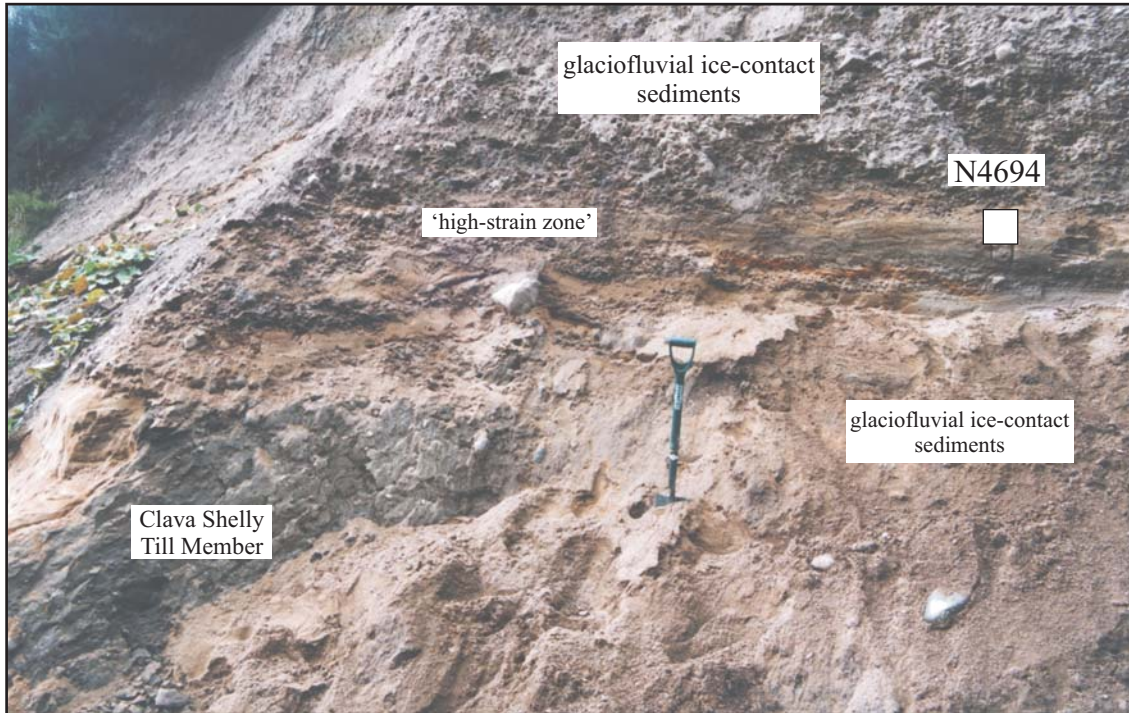
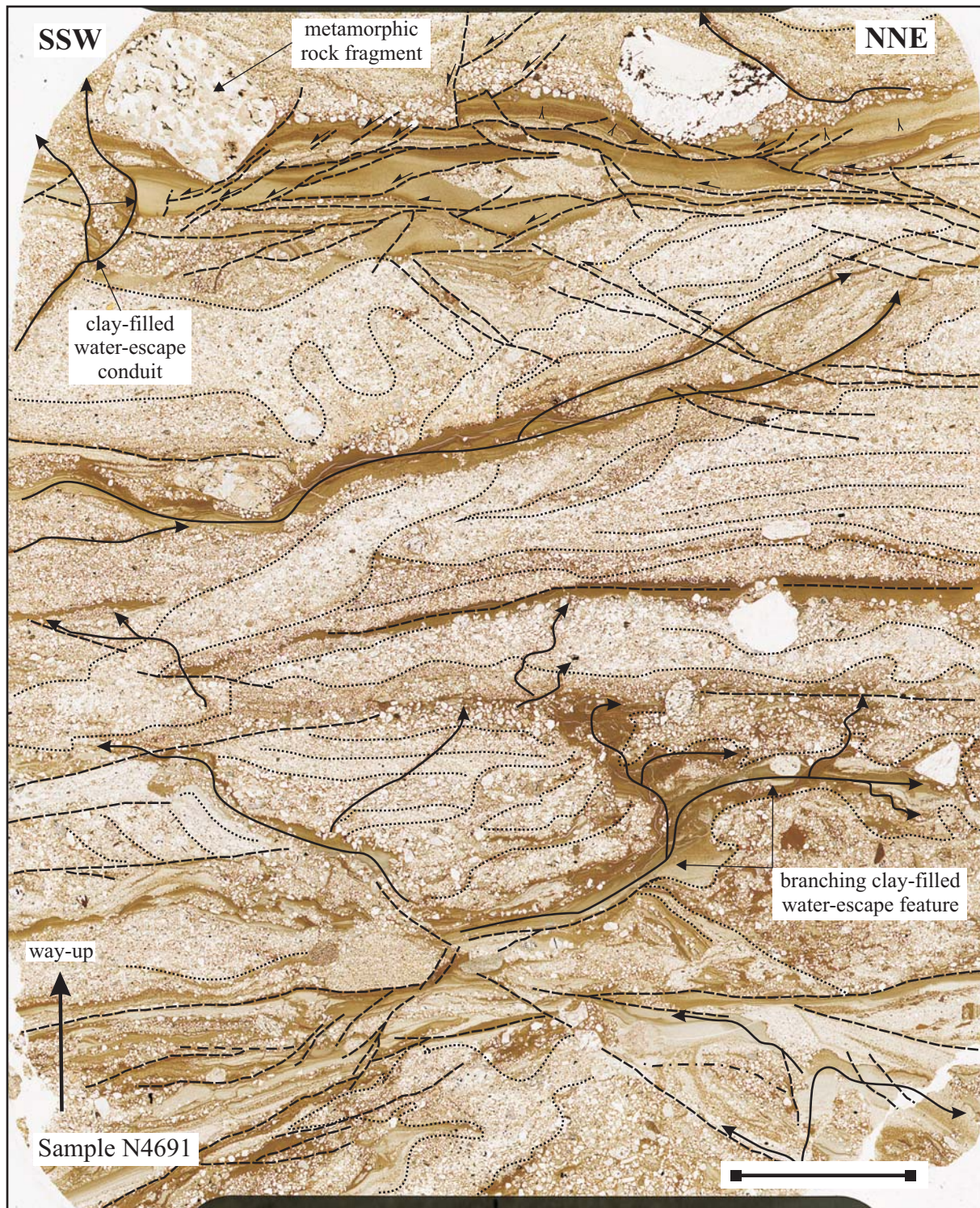


Figure 5. Photograph of a clay-rich high strain zone marking a thrust deforming the glaciofluvial deposits exposed in the stream section west of Drummore of Clava. The location of sample N4691 (QX194) is also shown.



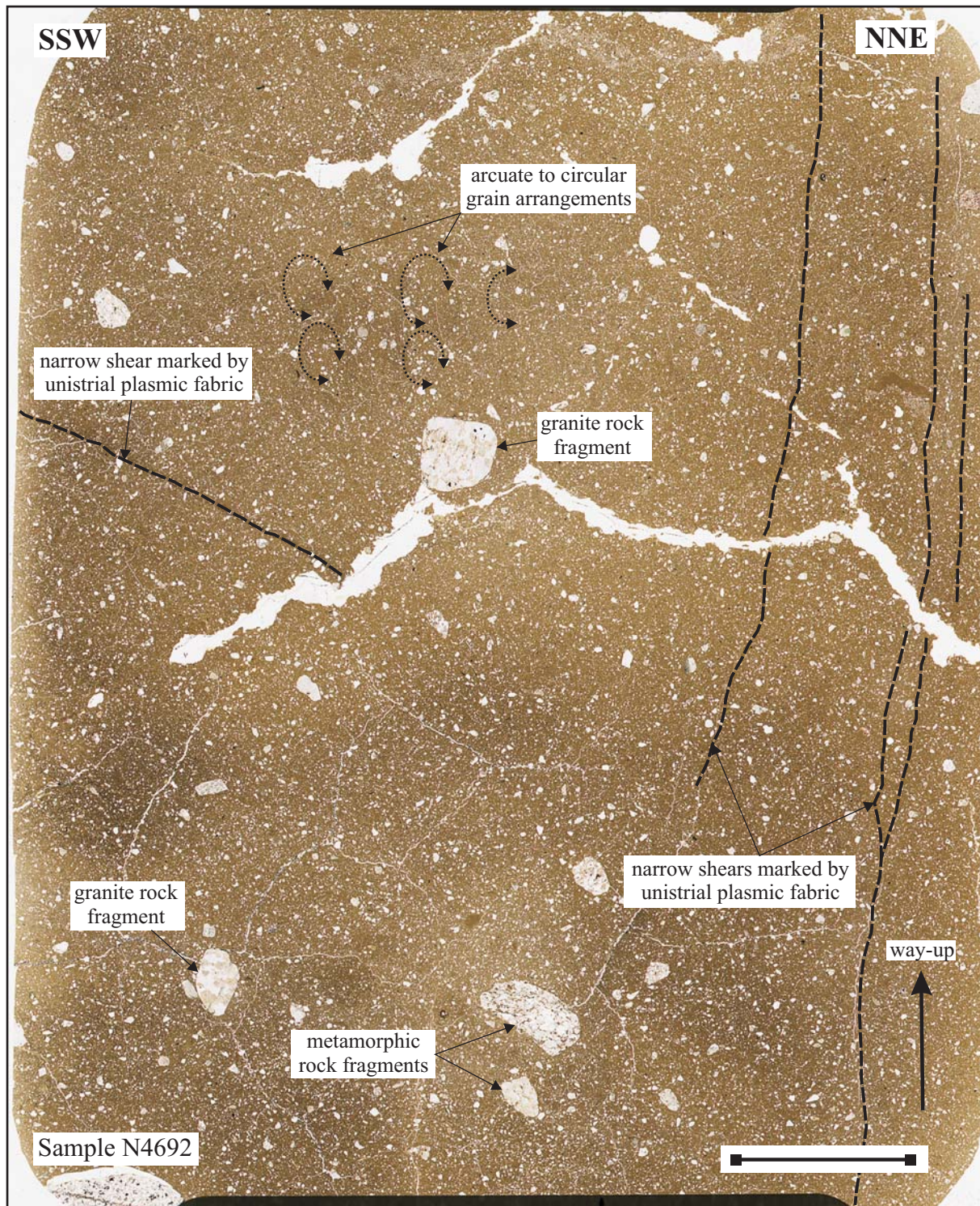
 thrusts and faults
  lithological boundaries
  water-escape features

Figure 6. Annotated scan of thin section N4691 (QX194) showing main structures developed within this deformed, laminated sand, silt and clay (Scale bar = 10 mm).

layer-parallel t
faulting conce
clay-rich layer

cross-cutting r
between indivi
sand, silt and c

complex cross
relationships b
irregular, fluid
and clay layers
branching, cla
water-escape c



 arcuate to circular grain arrangements
  narrow shears marked by unistrial plasmic fabric

Figure 7. Annotated scan of thin section N4692 (QX195) showing main structures developed within this diamicton, Clava Shelly Till Member (Scale bar = 10 mm).

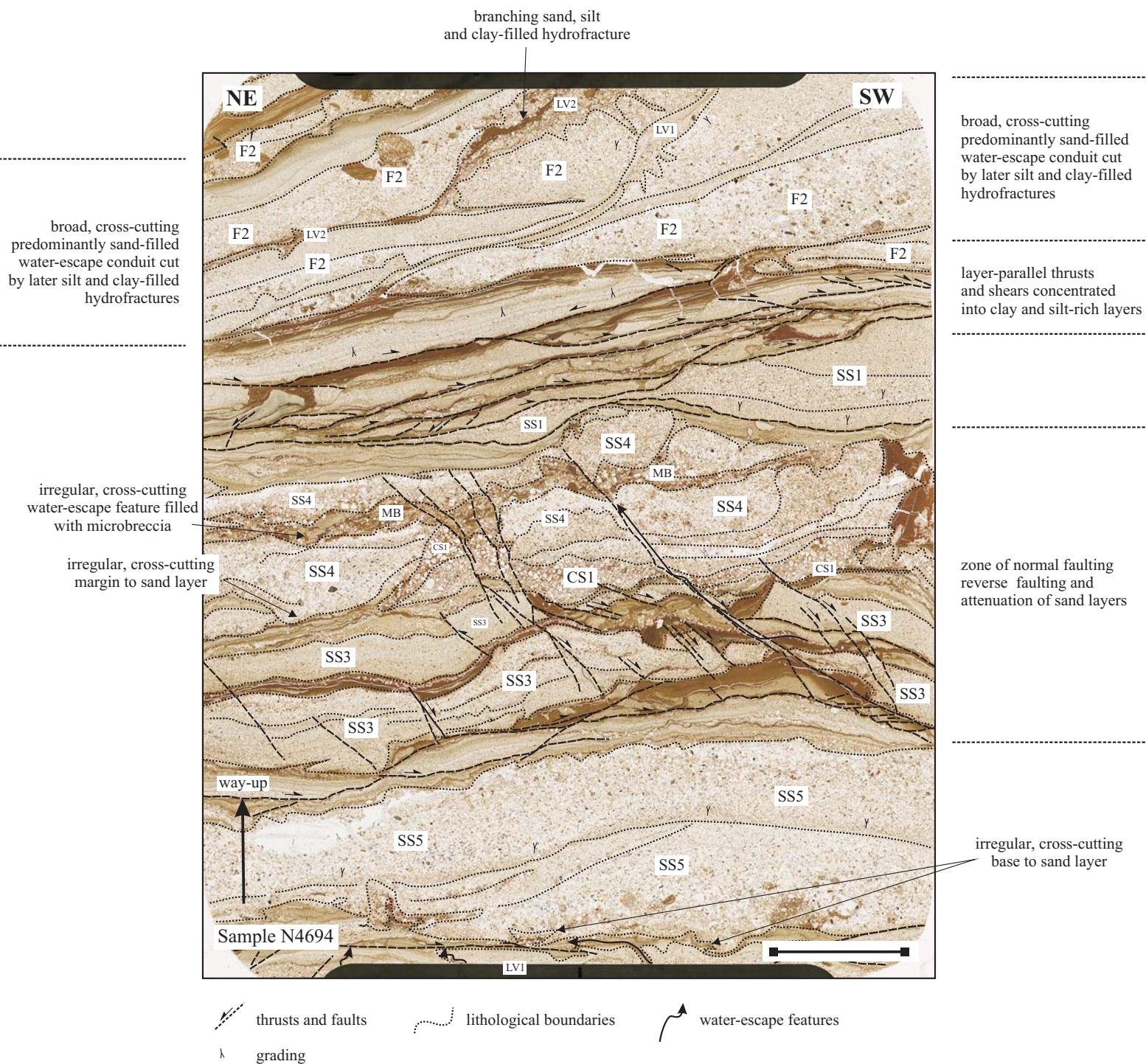


Figure 9. Annotated scan of thin section N4694 (QX197) showing main structures developed within this deformed, laminated sand, silt and clay, Clava Sand Member (Scale bar = 10 mm).

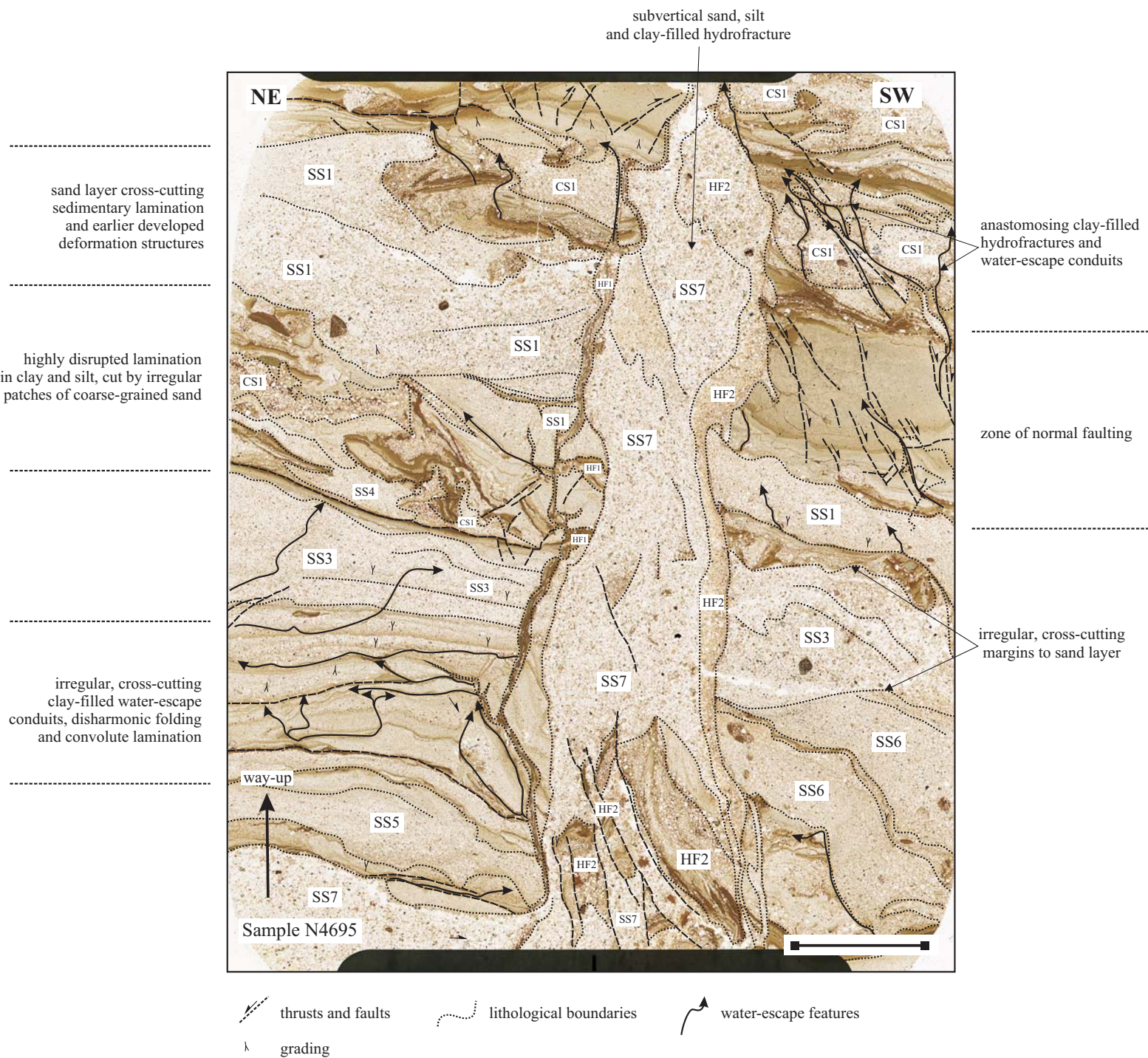


Figure 10. Annotated scan of thin section N4695 (QX198) showing main structures developed within this deformed, laminated sand, silt and clay, Clava Sand Member. Most prominent structure is a steeply dipping sand, silt and clay-filled hydrofracture system (Scale bar = 10 mm).

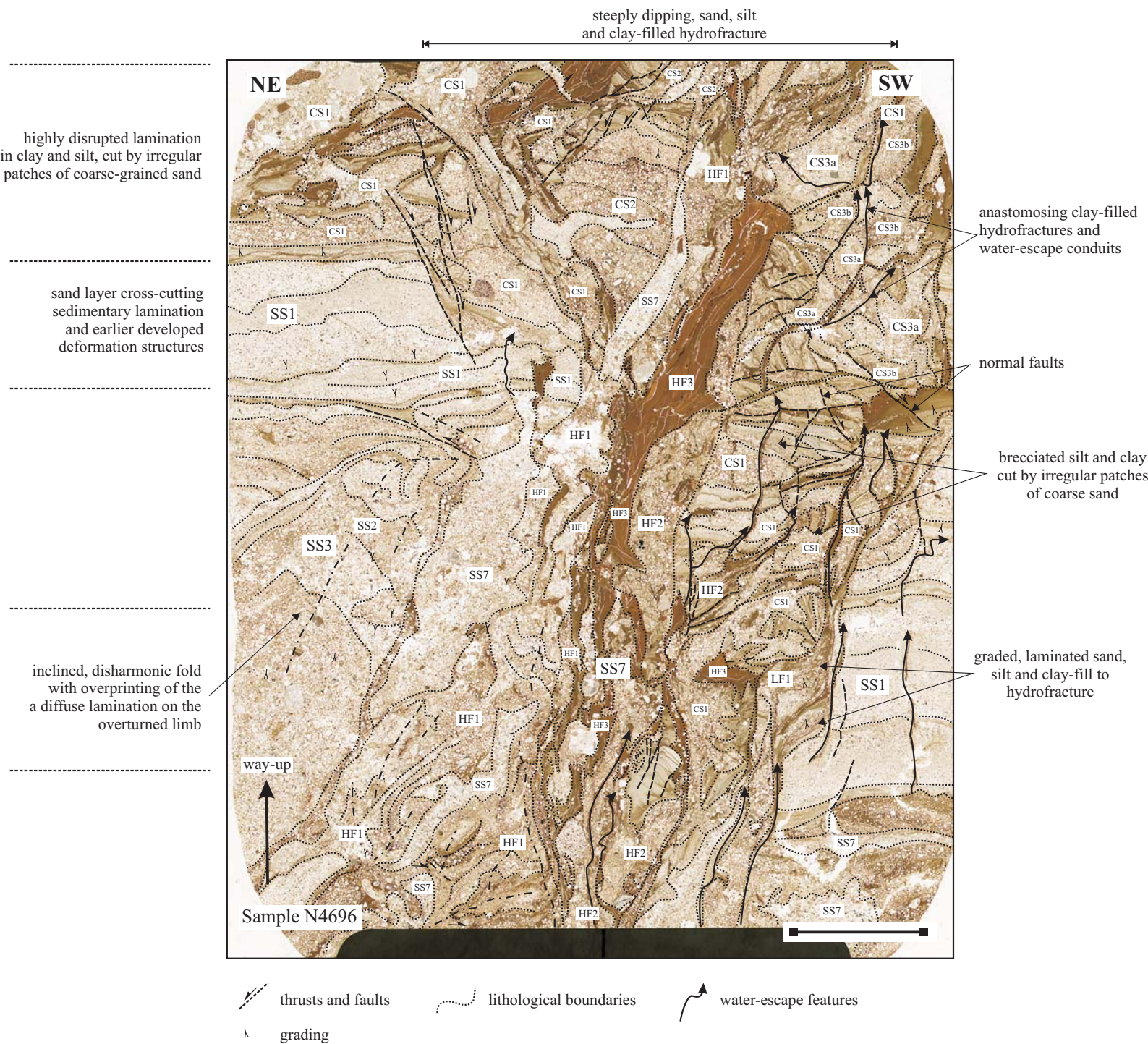


Figure 11. Annotated scan of thin section N4696 (QX200) showing main structures developed within this deformed, laminated sand, silt and clay, Clava Sand Member. Most prominent structure in this highly brecciated sample is a funnel-shaped, steeply dipping sand, clay and silt-filled hydrofracture system (Scale bar = 10 mm).